Available online at www.sciencedirect.com
ScienceDirect
Journal of Computational Physics 223 (2007) 657–684
JOURNAL OF COMPUTATIONAL PHYSICS
www.elsevier.com/locate/jcp

Optimal control of the free boundary in a two-phase Stefan problem

Michael Hinze [a,*], Stefan Ziegenbalg [b]

[a] University of Hamburg, Department of Mathematics, D-20146 Hamburg, Bundesstrasse 55, Germany
[b] TU-Dresden, Institute of Mathematics, D-01062 Dresden, Zellescher Weg 12-14, Germany

Received 15 November 2005; received in revised form 28 September 2006; accepted 29 September 2006
Available online 28 November 2006

Abstract

We present an optimal control approach for the solidification process of a melt in a container. The process is described by a two phase Stefan problem with the free boundary (interface between the two phases) modelled as a graph. We control the evolution of the free boundary using the temperature on the container wall. The control goal consists in tracking a prescribed evolution of the free boundary. We achieve this goal by minimizing a appropriate cost functional. The resulting minimization problem is solved numerically by a steepest descent method with step size control, where the gradient of the cost functional is expressed in terms of the adjoint variables. Several numerical examples are presented which illustrate the performance of the method.

The novelty of the approach presented consists in using a sharp interface model for the control of the free boundary. This guarantees direct access to the free boundary as optimization variable in terms of its parametrization as a graph. Moreover at any stage of the optimization process the physical laws constituted by the mathematical model are conserved, and the heat flux into the free boundary is variable and thus does not need to be specified a priori in the optimization process. This guarantees more flexibility than in the optimization approaches to two phase Stefan problems taken so far.

PACS: 02.30.Yy; 44.35.+c; 64.70.Dv

Keywords: Solidification; Control; Stefan condition; Adjoint approach

1. Introduction

Solidification processes play an important role in many areas of metallurgy. For example, in many crystal growth processes the evolution and the form of the interface between the solid and liquid phase strongly influences the quality of the crystal. It is known from engineering experience, that certain forms of interfaces (flat, concave, convex) exclude dislocations, say and thus enhance material properties.

* Corresponding author. Tel.: +49 351 463 37584; fax: +49 351 463 34268.
E-mail addresses: michael.hinze@uni-hamburg.de (M. Hinze), stefan.ziegenbalg@tu-dresden.de (S. Ziegenbalg).

0021-9991/$ - see front matter
doi:10.1016/j.jcp.2006.09.030

In the present work we develop an optimization strategy for the free boundary in a two phase Stefan problem. As mathematical model we use heat conduction in the two phases, where the coupling of the phases is established through the Stefan condition at the free boundary. We use a sharp interface model and assume that the free boundary can be described by a graph. Our goal is to control the evolution of the free boundary using the temperature on the container boundary as control function. Control through boundary temperature is a macroscopic control mechanism. Considering this, we neglect effects on the meso- and microscale, such as dendritic growth and the evolution of point defects, in our mathematical model. To achieve the control goal we track a prescribed evolution of the interface which from the optimization point of view serves as desired state. For this purpose we define a cost functional in which the error between the graphs of the free boundary and a desired free boundary is to be minimized. The modeling of the interface as a graph is motivated by the ability to access directly the free boundary in terms of an optimization variable. To anticipate discussions we note that the incorporation of meso- and microscopic effects would necessitate a different modelling of the interface.

Altogether we end up with an optimization problem for the temperature on the container wall, which is coupled to the temperature in the solid and liquid phases and to the desired free boundary by an highly nonlinear system of pde's.

To the best of our knowledge this is the first attempt to control the evolution of the free boundary directly using a sharp interface model. With the approach presented we advance simulation and optimization capabilities in solidification processes in the following respects; the interface serves as an optimization variable itself and thus can be controlled directly. This is different for control of the free boundary in phase field and level set models where the free boundary is diffuse or represented as a zero level set, respectively, so that it only admits indirect control. Furthermore at any stage of the optimization process the physical laws constituted by our mathematical model are conserved. This among other things guarantees that every solution to our optimization problem consisting of the interface and the states in the solid and liquid phases, is physical in the sense that it obeys the physics constituted by the mathematical model.

Let us first comment on closely related literature in this research field. Zabaras et al. in [18,20,7,19,16,17] consider an approach where the free boundary is assumed to be known a-priori. In [18] a one-dimensional problem is considered. The heat flow into the free boundary and the position of the free boundary is given and the heat flow into the fixed boundary is to be determined. In particular, in both phases an inverse heat conduction equation is solved using a integral method such that the melting temperature condition $\vartheta = \vartheta_m$ is satisfied at the free boundary, where ϑ is the temperature and ϑ_m is the melting temperature.

In [7,19] the inverse problem is replaced by a minimization problem. Its goal consists in minimizing the temperature difference at the free boundary, i.e. $\frac{1}{2}\|\vartheta_m - \vartheta(x,t)\|^2_{L_2(\Gamma\times[0,T])} = \min_{q_0}$, where q_0 is the heat flow into the solid phase at the fixed boundary. This means that the free boundary is set to the desired boundary without ensuring that the melting temperature condition $\vartheta = \vartheta_m$ is satisfied at the free boundary. A-priori fixing of the free boundary also implies, that the Stefan condition is applied at a wrong position (namely not at the real free boundary) and that the wrong physical constants for the heat equation in the area between the real free boundary and the desired free boundary are used. The heat flow at the fixed boundary into the liquid phase is set to 0 (this means, that the container is isolated). This allows to separate the problems for each phase. In particular, the heat flow into the free boundary can be computed using the Stefan condition, and by solving a direct (forward) heat conduction problem [7], or a direct (forward) heat conduction problem including convection [19]. The optimization goal consists in determining the heat flux at the fixed boundary of the solid phase and is solved by a conjugated gradient algorithm, where the sensitives are determined using the adjoint approach.

Yang in [16] extends the approach of [19] to the case where the temperature at the fixed boundary in the liquid phase is also variable. To separate the problems for each phase the heat flux into the free boundary is assumed to be given. The minimization problem in the liquid phase consists in determining the temperature at the fixed boundary considering heat conduction, convection and the Stefan condition, such that the error of the temperature at the free boundary $\|\vartheta_m - \vartheta(x,t)\|^2_{L_2(\Gamma\times[0,T])}$ is minimized, with the position of the free boundary and heat flux into the free boundary given. The minimization problem for the solid phase then reads as in [7,19]: Given the position and the heat flux of the free boundary, find the heat flux on the fixed boundary such that the error of the temperature at the free boundary is minimized.

Let us comment more detailed on the differences of our approach compared to those presented by Kang and Zabaras in [7], Zabaras and Nguyen in [19], and Yang in [16]. In these approaches the heat flux into the free boundary needs to be specified a-priori in the optimization problem. This is unusual since in an optimization approach to a Stefan problem the heat flux into the free boundary should be variable and not be specified a-priori. Zabaras et al. resolve this problem by fixing the heat flux into the liquid phase (see above). As a consequence only the heat flux into the solid phase may serve as control variable in his approach. This is different in the approach presented here, where the heat fluxes into both, the liquid and the solid phase are variable and therefore may serve as control variables. This in turn gives further flexibility in the optimization process. Yang fixes the heat flux into the free boundary a-priori, which is usually unknown in practice. As already mentioned above, both, the approach of Zabaras et al. and Yang have in common that the free boundary is a-priori fixed so that the Stefan condition probably is applied at a wrong position and the underlying physics is not longer represented by the mathematical model. Speaking in mathematical terms their approach only guarantees a physical solution ϑ if $\|\vartheta_{\mathrm{m}} - \vartheta(x,t)\|^2_{L_2(\Gamma\times[0,T])} = 0$ is satisfied which for a-priori fixed free boundaries certainly only happens by chance. We recall that in the approach presented here every solution is guaranteed to satisfy the mathematical system which certainly forms an advantage compared to the approaches sketched above.

Let us also briefly comment on further literature related to our research. In [3] the free boundary is controlled by thermostats acting on the boundary. Instead of optimal control a feedback control based on real temperature measurements is applied. As mathematical model a hyperbolic Stefan problem based on the linearized Gurtin–Pipkin heat conduction law is used. In [6] a one-dimensional two-phase Stefan problem with "on–off" control is analyzed.

In [5,4] free boundary control is performed by inversion of the one-dimensional Stefan problem with a quadratic nonlinear reaction term. Kearsley in [8] controls the amount of melted material for a Stefan problem using a sequential quadratic programming algorithm.

Pawlow in [10,11] presents an approach, where the error between a desired temperature ϑ_{d} and the temperature of the substance is to be minimized over the whole space–time domain using boundary control. She considers a two-phase Stefan problem which is transformed into a variational inequality, and also develops an efficient gradient type algorithm based on the adjoint system approach.

The present paper is organized as follows. Section 2 contains the problem specification including the physical model and the optimization problem. Further an expression for the gradient of the cost functional is presented which uses adjoint information. Section 3 contains the description of the numerical approach taken in the present work, including a detailed discussion of the optimization algorithm. Section 4 presents numerical results for the solidification of a silicon melt, and the Appendix contains a detailed derivation of the adjoint system and of the compatibility conditions of the boundary temperature at the intersection of the container wall and the free boundary.

2. Problem definition

2.1. Physical model

Let $\Omega \subset \mathbb{R}^{n+1}$ be a bounded domain containing the substance. For $t \in [0,T]$ let $\Omega_{\mathrm{s}}(t), \Omega_{\mathrm{l}}(t) \subset \Omega$ denote the parts containing the solid and the liquid phase, where $\Omega_{\mathrm{s}}(t) \cap \Omega_{\mathrm{l}}(t) = \emptyset$ and $\overline{\Omega} = \overline{\Omega_{\mathrm{s}}(t)} \cup \overline{\Omega_{\mathrm{l}}(t)}$. The free boundary is n-dimensional and defined by $\Gamma(t) = \overline{\Omega_{\mathrm{s}}(t)} \cap \overline{\Omega_{\mathrm{l}}(t)}$, see Fig. 1 for $n = 1$.

In each phase the heat equation for the absolute temperature holds;

$$\partial_t \vartheta = \frac{k_{\mathrm{s}}}{c_{\mathrm{s}}\rho_{\mathrm{s}}}\Delta\vartheta \quad \text{in } \Omega_{\mathrm{s}}, \qquad \partial_t \vartheta = \frac{k_{\mathrm{l}}}{c_{\mathrm{l}}\rho_{\mathrm{l}}}\Delta\vartheta \quad \text{in } \Omega_{\mathrm{l}}. \tag{1}$$

Here k_{s}, k_{l} are the heat conductivities in the solid and liquid phase, respectively, c_{s}, c_{l} denote the specific heat capacities, and ρ_{s}, ρ_{l} the corresponding densities.

The Stefan condition is a conservation law on the free boundary which balances the heat transported into the free boundary and the melting heat generated through solidification. In mathematical terms it reads

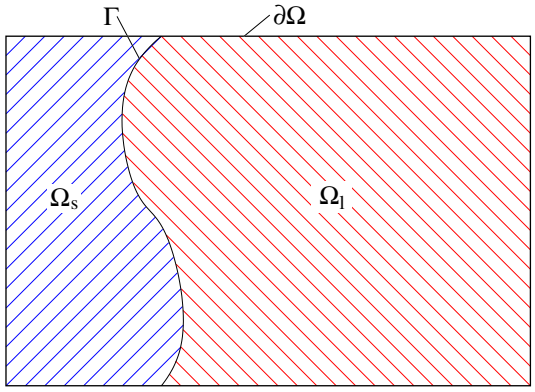

Fig. 1. Solid phase Ω_s, liquid phase Ω_l and free boundary Γ in a container with boundary $\partial\Omega$.

$$V_\Gamma(L_l - L_s) = \frac{k_s}{\rho_s}\partial_\mu\vartheta\Big|_{\Omega_s} - \frac{k_l}{\rho_l}\partial_\mu\vartheta\Big|_{\Omega_l} =: -\left[\frac{k_{s/l}}{\rho_{s/l}}\partial_\mu\vartheta\right]_\Gamma \quad \text{on } \Gamma. \tag{2}$$

Here μ denotes the unit normal vector of the free boundary, directed from the solid into the liquid phase. V_Γ is the velocity in direction of μ and L is the latent heat per unit volume in each of the phases. The right hand side of (2) describes the heat transported into the boundary and the left hand side describes the (melting) heat which is generated by the solidification, see [9,15,8] for a description of this model.

At the free boundary Γ the temperature satisfies

$$\vartheta = \vartheta_M, \tag{3}$$

where ϑ_M denotes the melting temperature.

The temperature ϑ_b of the container is coupled to the temperature at the phase boundaries through the heat transfer equation

$$q = \alpha_{s/l}(\vartheta_b - \vartheta) \quad \text{on } \partial\Omega_{s/l},$$

where the heat flow density q is given by $q = k_{s/l}\partial_\nu\vartheta$. ($\alpha = 0$ would refer to the case that the container is isolated.) This leads to a third-order boundary condition of the form

$$\vartheta + \frac{k_{s/l}}{\alpha_{s/l}}\partial_\nu\vartheta = \vartheta_b \quad \text{on } \partial\Omega, \tag{4}$$

where ν is the outer normal vector of the boundary $\partial\Omega$, i.e. $\mu = \nu|_{\partial\Omega_s} = -\nu|_{\partial\Omega_l}$ on Γ.

To avoid problems with mass conservation we assume $\rho_l = \rho_s = \rho$, which forms no real restriction since in most practical applications the density in solid and liquid phase is approximately equal. We set $u := \frac{\vartheta - \vartheta_M}{\rho(L_l - L_s)}$ and $D_{s/l} := \frac{k_{s/l}}{c_{s/l}\rho}$ so that Eqs. (1)–(4) transform into

$$\begin{aligned}
&\partial_t u = D_{s/l}\Delta u \quad \text{in } \Omega_{s/l},\\
&V_\Gamma = -[k_{s/l}\partial_\mu u]_\Gamma \quad \text{on } \Gamma,\\
&u = 0 \quad \text{on } \Gamma,\\
&u_b = u + \frac{k_{s/l}}{\alpha_{s/l}}\partial_\nu u \quad \text{on } \partial\Omega.
\end{aligned}$$

As initial value conditions we now have

$$\begin{aligned}
&u(0,x) = u_0(x) \quad \text{in } \Omega \text{ and}\\
&\Gamma(0) = \Gamma_0.
\end{aligned}$$

2.2. Optimization problem

Our goal is to control the free boundary using the boundary temperature $u_b(t,x)$ on the container walls. As control horizon we take $t \in (0,T]$ for some $T > 0$. We split u_b into two parts:

$$u_b = u_{b0} + \beta u_{bc},$$

with a fixed part u_{b0} (e.g. a temperature known from experience), and a control temperature part βu_{bc}, where β is a weight function which allows to tailor the control part of the boundary condition.

The domain is assumed a-priori known to be a container of the form $\Omega = (0,X_1)\times(0,X_2)\times\cdots\times(0,X_{n+1})$. The free boundary is described as a graph

$$\Gamma(t) = \left\{ \begin{pmatrix} y \\ f(t,y) \end{pmatrix} : y \in [0,X_1]\times\cdots\times[0,X_n] \right\},$$

with $f : [0,T]\times[0,X_1]\times\cdots\times[0,X_n] \to [0,X_{n+1}]$. For the ease of notation we define $S := [0,X_1]\times\cdots\times[0,X_n]$.

We model the desired evolution $\overline{\Gamma}$ also as a graph by $\bar{f} : [0,T]\times S \to [0,X_{n+1}]$, and then are in the position to formulate the objective functional of our minimization problem;

$$\begin{aligned} J(f,u_{bc}) &:= \frac{1}{2}\int_0^T \int_S (f(t,y)-\bar{f}(t,y))^2 \mathrm{d}y\,\mathrm{d}t + \frac{\lambda_2}{2}\int_S (f(T,y)-\bar{f}(T,y))^2 \mathrm{d}y \\ &\quad + \frac{\lambda_1}{2}\int_0^T \int_{\partial\Omega} \beta(t,x)^2 u_{bc}(t,x)^2 \mathrm{d}x\,\mathrm{d}t \\ &= \min !_{u_{bc}}. \end{aligned} \tag{5}$$

The first two terms in this expression model the objective in our minimization problem with λ_2 weighing the deviation of the free boundary from the desired free boundary at time $t = T$. The third term weighs the control cost with λ_1 and may serve as regularization.

2.3. The two dimensional case

Next we develop equations for the velocity of a graph in the two-dimensional case ($n = 1$). The tangential vector of the graph

$$\Gamma(t) = \left\{ \begin{pmatrix} y \\ f(t,y) \end{pmatrix} : y \in [0,X_1] \right\},$$

at the point y is given by $(\,1 \quad f_y(t,y)\,)^{\mathrm{T}}$, and the normal μ can be expressed as

$$\mu(t,y) = \frac{1}{\sqrt{1+f_y(t,y)^2}} \begin{pmatrix} -f_y(t,y) \\ 1 \end{pmatrix}.$$

For the velocity of the graph in normal direction we obtain

$$V_\Gamma(t,y) := \frac{\partial}{\partial t}\begin{pmatrix} y \\ f(t,y) \end{pmatrix}^{\mathrm{T}} \mu(t,y) = \frac{1}{\sqrt{1+f_y(t,y)^2}} \begin{pmatrix} 0 \\ f_t(t,y) \end{pmatrix}^{\mathrm{T}} \begin{pmatrix} -f_y(t,y) \\ 1 \end{pmatrix} = \frac{f_t(t,y)}{\sqrt{1+f_y(t,y)^2}}. \tag{6}$$

Next we specify the initial and boundary conditions for f. For this purpose we recall that $\bar{f}$ denotes the desired evolution of the free boundary. As initial condition we set $f(0,y) = \bar{f}(0,y)$ and define $f_0(y) := \bar{f}(0,y)$. Moreover we introduce the following boundary condition for f:

$$f(t,0) = \bar{f}(t,0), \quad f(t,X_1) = \bar{f}(t,X_1). \tag{7}$$

Besides the fact that we intend to incorporate as much a-priori information as possible into our mathematical model, this choice simplifies our moving grid implementation. Especially it avoids the need of an additional boundary grid for the boundary temperature, and this avoids the interpolation of its values between the two grids. Further details are given in Section 3.5.

To ensure continuity at the intersection of the container wall and the free boundary the introduction of (7) requires the following compatibility conditions for u_b, whose detailed derivation is presented in Appendix B;

$$\frac{\bar{f}_t f_y}{1+f_y^2} = (\alpha_s - \alpha_l)u_b \quad \text{on } (0,T]\times\{(0,\bar{f}(t,0))\}, \tag{8}$$

$$\frac{\bar{f}_t f_y}{1+f_y^2} = -(\alpha_s - \alpha_l)u_b \quad \text{on } (0,T]\times\{(X_1,\bar{f}(t,X_1))\}. \tag{9}$$

Since f_y is unknown we also specify f_y with the help of $\bar{f}$ as follows:

$$f_y(t,0) = \bar{f}_y(t,0), \quad f_y(t,X_1) = \bar{f}_y(t,X_1). \tag{10}$$

The continuity of our system finally leads to

$$\partial_{e_2} u_b|_{\Omega_{s/l}} = \frac{\bar{f}_t}{1+\bar{f}_y^2}\left(\frac{1}{\alpha_s-\alpha_l}\left(\frac{\alpha_{s/l}}{k_{s/l}} + 2\frac{\bar{f}_y f_{yy}}{(1+\bar{f}_y^2)^2}\right) - \frac{u_b}{D_{s/l}}\right) - \frac{\bar{f}_{yt}}{(\alpha_s-\alpha_l)(1+\bar{f}_y^2)^2} \tag{11}$$

on $(0,T]\times\{(0,f(t,0))\}$, and

$$\partial_{e_2} u_b|_{\Omega_{s/l}} = \frac{\bar{f}_t}{1+\bar{f}_y^2}\left(\frac{1}{\alpha_s-\alpha_l}\left(\frac{\alpha_{s/l}}{k_{s/l}} - 2\frac{\bar{f}_y f_{yy}}{(1+\bar{f}_y^2)^2}\right) - \frac{u_b}{D_{s/l}}\right) + \frac{\bar{f}_{yt}}{(\alpha_s-\alpha_l)(1+\bar{f}_y^2)^2} \tag{12}$$

on $(0,T]\times\{(X_1,f(t,X_1))\}$. Since f_{yy} is unknown in these equations we further set

$$f_{yy}(t,0) = \bar{f}_{yy}(t,0), \quad f_{yy}(t,X_1) = \bar{f}_{yy}(t,X_1). \tag{13}$$

Appendix B contains a detailed derivation of these compatibility conditions. To anticipate the discussion of Section 3.5 we note, that these boundary conditions are motivated mathematically. In particular they simplify the numerical implementation.

Further we need to ensure that the boundary condition is satisfied for $t=0$, i.e. we need to set

$$u_b(0,x) = u_0(x) + \frac{k_{s/l}}{\alpha_{s/l}}\partial_\nu u_0(x). \tag{14}$$

We recall that the temperature u_b on the container wall is split into two parts, i.e. $u_b = u_{b0} + \beta u_{bc}$. Now we require that u_{b0} satisfies the compatibility conditions (8), (9), (11), (12) and (14) and assume

$$\begin{aligned} &\beta(t,x) = \partial_{e_2}\beta(t,x) = 0 \quad \text{for } x\in\Gamma\cap\partial\Omega \text{ and } t\in(0,T],\\ &\beta(0,x) = 0 \quad \text{for } x\in\partial\Omega. \end{aligned} \tag{15}$$

These conditions ensure that u_b for every choice u_{bc} satisfies (8), (9), (11), (12) and (14), so that u_{bc} may serve as the control variable in our optimization problem specified below. Particular choices for β are presented in Section 4.1.

Our optimization problem now reads

$$\begin{aligned} J(f,u_{bc}) :=& \frac{1}{2}\int_0^T\int_0^{X_1}(f(t,y)-\bar{f}(t,y))^2\mathrm{d}y\,\mathrm{d}t + \frac{\lambda_1}{2}\int_0^T\int_{\partial\Omega}\beta(t,x)^2 u_{bc}(t,x)^2\mathrm{d}x\,\mathrm{d}t\\ &+\frac{\lambda_2}{2}\int_0^{X_1}(f(T,y)-\bar{f}(T,y))^2\mathrm{d}y\\ =& \min!_{u,f,u_{bc}}, \end{aligned} \tag{16}$$

subject to the conditions

$$\partial_t u(t,x) - D_{s/l}\Delta u(t,x) = 0 \quad \text{for } t\in(0,T] \text{ and } x\in\Omega_{s/l}(t), \tag{17}$$

$$f_t(t,y) + \sqrt{1+f_y(t,x)}[k_{s/l}\partial_\mu u]\left(t,\begin{pmatrix} y\\ f(t,y)\end{pmatrix}\right) = 0 \quad \text{for } t\in(0,T] \text{ and } y\in(0,X_1), \tag{18}$$

$$u(t,x) = 0 \quad \text{for } x = \begin{pmatrix} y\\ f(t,y)\end{pmatrix},\ t\in(0,T] \text{ and } y\in(0,X_1), \tag{19}$$

$$\frac{k_{s/l}}{\alpha_{s/l}}\partial_\nu u(t,x) + u(t,x) - u_{b0}(t,x) - \beta(t,x)u_{bc}(t,x) = 0 \quad \text{for } t \in (0,T) \text{ and } x \in \partial\Omega_{s/l}(t) \setminus \Gamma(t), \tag{20}$$

$$u(0,x) = u_0(x) \quad \text{for } x \in \overline{\Omega}, \tag{21}$$

$$f(0,y) = \bar{f}(0,y) \quad \text{for } y \in [0,X_1], \text{ and} \tag{22}$$

$$\left.\begin{array}{ll} f(t,0) = \bar{f}(t,0) & f(t,X_1) = \bar{f}(t,X_1), \\ f_y(t,0) = \bar{f}_y(t,0) & f_y(t,X_1) = \bar{f}_y(t,X_1), \\ f_{yy}(t,0) = \bar{f}_{yy}(t,0) & f_{yy}(t,X_1) = \bar{f}_{yy}(t,X_1) \end{array}\right\} \quad \text{for } t \in (0,T]. \tag{23}$$

The functions u_{b0}, β, $\bar{f}$ and u_0 are given and the functions u, f, u_{bc} are sought. Eqs. (17)–(20) represent the heat equation, the Stefan condition, the condition for the melting temperature and the heat transfer condition at the boundary $\partial\Omega$. Eqs. (21)–(23) represent the initial and the boundary conditions for u and f. From here onwards we assume that the optimization problem admits a solution (u^*, f^*, u_{bc}^*).

2.4. Sensitives via the adjoint equation approach

We now formally derive the first-order necessary optimality condition for the minimization problem (16)–(23) using the Lagrange approach. The Lagrange functional associated to the minimization problem (16)–(20) is given by

$$\begin{aligned} &L(f,u,u_{bc},p_s,p_l,p_{bs},p_{bl},p_{\Gamma,1},p_{\Gamma,2}) \\ &\quad := J(f,u_{bc}) + \int_0^T \int_{\Omega_s} (\partial_t u - D_s\Delta u)p_s + \int_0^T \int_{\Omega_l} (\partial_t u - D_l\Delta u)p_l \\ &\qquad + \int_0^T \int_0^{X_1} \left(\sqrt{1+f_y^2}[k_{s/l}\partial_\mu u]\circ\Phi + f_t\right)p_{\Gamma,1} + \int_0^T \int_0^{X_1} (u\circ\Phi)p_{\Gamma,2} \\ &\qquad + \int_0^T \int_{\partial\Omega_s(t)\setminus\Gamma(t)} \left(\frac{k_s}{\alpha_s}\partial_\nu u + u - u_{b0} - \beta u_{bc}\right)p_{bs} + \int_0^T \int_{\partial\Omega_l(t)\setminus\Gamma(t)} \left(\frac{k_l}{\alpha_l}\partial_\nu u + u - u_{b0} - \beta u_{bc}\right)p_{bl}, \end{aligned}$$

where u and f are required to satisfy (21)–(23), and with

$$\Phi(t,y) := \left(t, \begin{pmatrix} y \\ f(t,y) \end{pmatrix}\right).$$

The functions p_s, p_l, p_{bs}, p_{bl}, $p_{\Gamma,1}$ and $p_{\Gamma,2}$ denote the Lagrange multipliers associated to (17)–(20). The first-order necessary optimality condition for our optimization problem now is given by

$$\nabla L = 0, \tag{24}$$

and the adjoint equation system for our problem is defined through

$$L_u\tilde{u} = 0 \quad \text{and} \quad L_f\tilde{f} = 0$$

for all feasible directions $\tilde{u}$ and $\tilde{f}$. (L_u and L_f here denote the directional derivatives of L with respect to u and f, respectively.) Using the normalizations

$$p_s = \frac{k_s}{D_s}q_s \quad \text{on } \Omega_s, \quad p_l = \frac{k_l}{D_l}q_l \quad \text{on } \Omega_l, \quad q_\Gamma = -p_{\Gamma,1}, \tag{25}$$

these conditions lead to the following adjoint equation system:

$$\left.\begin{array}{l} \partial_t q_s(t,x) + D_s\Delta q_s(t,x) = 0 \\ \partial_t q_l(t,x) + D_l\Delta q_l(t,x) = 0 \end{array}\right\} \quad \text{for} \quad \begin{array}{l} x \in \Omega_s(t) \\ x \in \Omega_l(t) \end{array} \quad \text{and } t \in (0,T), \tag{26}$$

$$\left.\begin{array}{l} q_s(t,x) = -\frac{k_s}{\alpha_s}\partial_\nu q_s(t,x) \\ q_l(t,x) = -\frac{k_l}{\alpha_l}\partial_\nu q_l(t,x) \end{array}\right\} \quad \text{for} \quad \begin{array}{l} x \in \partial\Omega_s(t) \setminus \Gamma(t) \\ x \in \partial\Omega_l(t) \setminus \Gamma(t) \end{array} \quad \text{and } t \in (0,T), \tag{27}$$

$$\begin{aligned} p_{\mathrm{bs}}(t,x) &= \alpha_{\mathrm{s}} q_{\mathrm{s}}(t,x) \\ p_{\mathrm{bl}}(t,x) &= \alpha_{\mathrm{l}} q_{\mathrm{l}}(t,x) \end{aligned} \quad \text{for} \quad \begin{aligned} x &\in \partial\Omega_{\mathrm{s}}(t) \setminus \Gamma(t) \\ x &\in \partial\Omega_{\mathrm{l}}(t) \setminus \Gamma(t) \end{aligned} \quad \text{and } t \in (0,T), \tag{28}$$

$$\begin{aligned} q_{\mathrm{s}}(T) &= 0 \\ q_{\mathrm{l}}(T) &= 0 \end{aligned} \quad \text{for} \quad \begin{aligned} x &\in \Omega_{\mathrm{s}}(t), \\ x &\in \Omega_{\mathrm{l}}(t), \end{aligned} \tag{29}$$

$$q_{\mathrm{s}}(t,x) = q_{\Gamma}(t,y) \quad \text{for } t \in (0,t),\ y \in (0,X_1) \text{ and } x = \begin{pmatrix} y \\ f(t,y) \end{pmatrix}, \tag{30}$$

$$q_{\mathrm{l}}(t,x) = q_{\Gamma}(t,y) \quad \text{for } t \in (0,t),\ y \in (0,X_1) \text{ and } x = \begin{pmatrix} y \\ f(t,y) \end{pmatrix}, \tag{31}$$

$$-\partial_t q_{\Gamma}(t,y) = f(t,y) - \bar{f}(t,y) \quad \text{for } t \in (0,t),\ y \in (0,X_1) \text{ and } x = \begin{pmatrix} y \\ f(t,y) \end{pmatrix}, \tag{32}$$

$$q_{\Gamma}(T,y) = \lambda_2 (f(T,y) - \bar{f}(T,y)) \quad \text{for } y \in [0,X_1) \text{ and} \tag{33}$$

$$q_{\Gamma}(t,0) = q_{\Gamma}(t,X_1) = 0 \quad \text{for } t \in [0,t]. \tag{34}$$

Eqs. (26)–(31) are deduced from $L_u \tilde{u} = 0$. They describe a "backward heat equation" in each phase with homogeneous third-order boundary conditions on the container boundary and Dirichlet boundary conditions on the free boundary. The functions p_{s}, p_{l} are the adjoint temperatures in the phases, and p_{bs} and p_{bl} are the adjoint temperatures on the container boundary. The function p_{Γ} is the adjoint graph function and is determined by $L_u \tilde{u} = 0 \wedge L_f \tilde{f} = 0$, which leads to (32)–(34). This equations can be equivalently written as

$$q_{\Gamma}(t,y) = \lambda_2 (f(T,y) - \bar{f}(T,y)) + \int_T^t f(s,y) - \bar{f}(s,y) \mathrm{d}s.$$

Appendix A contains a detailed derivation of the adjoint equation system.

Now we assume that the Stefan problem for every u_{bc} admits a unique solution. In particular we consider f as a function of u_{bc}, $f = f(u_{\mathrm{bc}})$. With these assumptions it is meaningful to define the reduced cost functional

$$K(u_{\mathrm{bc}}) := J(f(u_{\mathrm{bc}}), u_{\mathrm{bc}}),$$

and it is well known, that

$$K'(u_{\mathrm{bc}}) = L_{u_{\mathrm{bc}}}(f, u, u_{\mathrm{bc}}, p_{\mathrm{s}}, p_{\mathrm{l}}, p_{\mathrm{bs}}, p_{\mathrm{bl}}, p_{\Gamma,1}, p_{\Gamma,2})$$

holds. Since here

$$L_{u_{\mathrm{bc}}}(f, u, u_{\mathrm{bc}}, p_{\mathrm{s}}, p_{\mathrm{l}}, p_{\mathrm{bs}}, p_{\mathrm{bl}}, p_{\Gamma,1}, p_{\Gamma,2})(t,x) = \lambda_1 \beta(t,x)^2 u_{\mathrm{bc}}(t,x) - \begin{cases} \beta p_{\mathrm{bs}}(t,x) & : \text{for } x \in \partial\Omega \setminus \partial\Omega_{\mathrm{l}}, \\ 0 & : \text{for } x \in \partial\Omega \cap \Gamma, \\ \beta p_{\mathrm{bl}}(t,x) & : \text{for } x \in \partial\Omega \setminus \partial\Omega_{\mathrm{s}}, \end{cases}$$

and all $t \in (0,T]$, there holds

$$K'(u_{\mathrm{bc}})(t,x) = \lambda_1 \beta(t,x)^2 u_{\mathrm{bc}}(t,x) - \begin{cases} \beta \alpha_{\mathrm{s}} q_s(t,x) & : \text{for } x \in \partial\Omega \setminus \partial\Omega_{\mathrm{l}}, \\ 0 & : \text{for } x \in \partial\Omega \cap \Gamma, \\ \beta \alpha_{\mathrm{l}} q_l(t,x) & : \text{for } x \in \partial\Omega \setminus \partial\Omega_{\mathrm{s}}, \end{cases} \tag{35}$$

where we have used (28). As a consequence the gradient $K'(u_{\mathrm{bc}})$ for given u_{bc} can be computed by first solving (17)–(23) for u, f, and then by solving (26)–(34) for the adjoint variables.

In our case the optimally condition (24) is equivalent to

$$K'(u_{\mathrm{bc}}) = 0. \tag{36}$$

In Section 3 we introduce a gradient method with line search to solve this equation numerically.

Remark 2.1. In practical applications pointwise bounds apply to boundary controls, i.e. $a \leqslant u_{\mathrm{bc}} \leqslant b$ has to hold with some functions a and b satisfying $a < b$. In this case the first-order necessary optimally condition reads

$$\int_0^T \int_{\partial\Omega} K'(u_{\mathrm{bc}})(t,x)(v(t,x)-u_{\mathrm{bc}}(t,x))\mathrm{d}x\,\mathrm{d}t \geqslant 0 \tag{37}$$

for all boundary functions v satisfying $a \leqslant v \leqslant b$.

3. The numerical approach

The algorithmical approach we take is an explicit finite difference approach on a moving grid on $\Omega = (0, X_1) \times (0, X_2)$. To be more precise we define the grid G at the time instance t by

$$G(t) := \{x_{ij}(t) : 0 \leqslant i \leqslant N_1; -N_2 \leqslant j \leqslant N_2\} \quad \text{with } x_{i,j}(t) = (x_{ij,1}(t), x_{ij,2}(t))$$

and fix the discretization in the first spatial direction (e_1-direction) by

$$x_{ij,1}(t) = y_i(t) = \begin{cases} \frac{X_1}{2}\left(1 - \left(1 - \frac{2i}{N_1}\right)^{\delta}\right) & : \frac{i}{N_1} < \frac{1}{2}, \\ \frac{X_1}{2}\left(1 + \left(\frac{2i}{N_1} - 1\right)^{\delta}\right) & : \frac{i}{N_1} \geqslant \frac{1}{2}, \end{cases} \tag{38}$$

where the parameter δ is used to adjust the grid width at the boundary, see Fig. 2. Practical values are $0.3 < \delta \leqslant 1$. The discretization of the second direction (e_2-direction) at $t = 0$ is defined by

$$x_{ij,2}(0) = \begin{cases} f_0(y_i)\left(1 + \frac{j}{N_2}\right) & : j < 0, \\ f_0(y_i)\left(1 - \frac{j}{N_2}\right) + X_2 \frac{j}{N_2} & : j \geqslant 0. \end{cases} \tag{39}$$

The polygon defined by the points $\{x_{i0}(0)\}$ is the discretized free boundary Γ_0.

For the time discretization we use the equidistant grid

$$\tau := \frac{T}{N_t}, \qquad t_l = l\tau, \quad l = 0, \ldots, N_t.$$

With $\hat{u}_{ij}(t_l)$ and $\hat{f}_i(t_l)$ the discrete temperature $\hat{u}_{ij}(t_l) \approx u(t_l, x_{ij}(t_l))$ and the discrete free boundary $\hat{f}_i(t_l) \approx f(t_l, y_i)$ are described. The discrete versions of the other variables are also supplemented with a hat.

For the numerical solution of the equation

$$K'(u_{\mathrm{bc}}) = 0,$$

we use the following gradient algorithm.

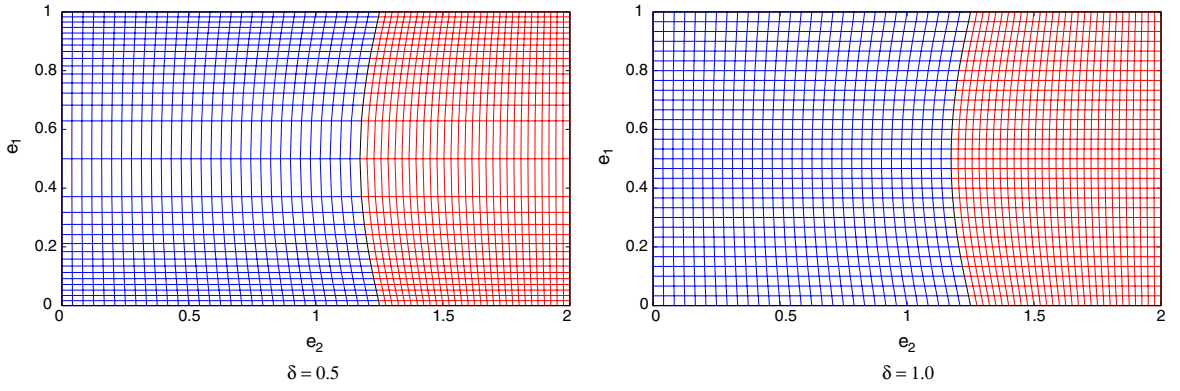

Fig. 2. Two grids with different parameters δ. Between the free boundary and the cylinder boundary the grid is equidistant in e_2-direction. For $\delta = 1$ it is also equidistant in e_1-direction.

C0: Initialization of $\hat{u}_{\mathrm{bc}}^{(0)}$:

$$\hat{u}_{\mathrm{bc},ij}^{(0)} = 0 \quad \text{for } i = 1, N_1 \text{ and } j = N_2+1,\dots,N_2-1,$$
$$\hat{u}_{\mathrm{bc},ij}^{(0)} = 0 \quad \text{for } |j| = N_2 \text{ and } i = 1,\dots,N_1-1.$$

FWD: Forward step 0: computation of $\hat{u}^{(0)}$, $\hat{f}^{(0)}$ using $\hat{u}_{\mathrm{bc}}^{(0)} = 0$
S1: For all $1 \leqslant k \leqslant k_{\max}$

BWD: Solving of the adjoint equation system
GRD: Computation of the gradient $\widehat{K}'(\hat{u}_{\mathrm{bc}}^{(k-1)}) =: \hat{v}^{(k)}$
LM: Line minimization: $\widehat{K}(\hat{u}_{\mathrm{bc}}^{(k-1)} + s^{(k)}\hat{v}^{(k)}) = \min !_{s^{(k)}}$
FWD: Forward step k: computation of $\hat{u}^{(k)}$, $\hat{f}^{(k)}$ using

$$\hat{u}_{\mathrm{bc}}^{(k)} = \hat{u}_{\mathrm{bc}}^{(k-1)} + s^{(k)}\hat{v}^{(k)}.$$

The particular steps are described in detail in the following subsections. Suitable stopping criterions are

$$k_{\max} := \min\left\{k : \frac{\widehat{J}^{(k-1)} - \widehat{J}^{(k)}}{\widehat{J}^{(0)}} \leqslant \varepsilon_J\right\} \tag{40}$$

and/or

$$k_{\max} := \min\left\{k : \frac{\|s^{(k)}\hat{v}^{(k)}\|}{\|u_{\mathrm{b0}}\|_2} \leqslant \varepsilon_v\right\}. \tag{41}$$

3.1. FWD: Forward step k

FWD.0: Initialization of the temperature $\hat{u}_{ij}^{(k)}(0) = u_0(x_{ij}^{(k)}(0))$ and of the grid, see (38) and (39)
FWD.1: For all $l = 1,\dots,N_t$

FWD.1.1 Computation of the motion of the free boundary using the Stefan condition:

$$\Delta\hat{f}_i^{(k)}(t_l) = (k_s\hat{\partial}_{e_2}^{-}u_{i0}^{(k)}(t_{l-1}) - k_l\hat{\partial}_{e_2}^{+}u_{i0}^{(k)}(t_{l-1}))(1+\hat{\partial}_y\hat{f}_i^{(k)}(t_{l-1})^2)\tau$$

for all $i = 1,\dots,N_1-1$, where $\hat{\partial}_{e_2}^{\mp}\hat{u}_{i0}^{(k)}(t_{l-1})$ denotes the finite backward/forward differences of $\partial_{e_2}u(t_{l-1}, x_{i0}^{(k)}(t_{l-1}))|_{\Omega_{s/l}}$. The discrete free boundary is equal to $\hat{f}_i^{(k)}(t_{l-1}) = \hat{x}_{i0,2}^{(k)}(t_{l-1})$, and $\hat{\partial}_y\hat{f}_i^{(k)}(t_{l-1})$ denotes the finite difference corresponding to $\partial_y f(t_{l-1}, y_i)$.Setting of the boundary values:

$$\Delta\hat{f}_0^{(k)}(t_l) := f_{\mathrm{b1}}(t_l) - f_{\mathrm{b1}}(t_{l-1}) \quad \Delta\hat{f}_{N_1}^{(k)}(t_l) := f_{\mathrm{b2}}(t_l) - f_{\mathrm{b2}}(t_{l-1}).$$

FWD.1.2 Computation of the new grid:

$$x_{ij,2}^{(k)}(t_l) = x_{ij,2}^{(k)}(t_{l-1}) + \Delta\hat{f}_i^{(k)}(t_l)\left(1 - \frac{|j|}{N_2}\right)$$

for all $i = 0,\dots,N_1$ and $j = -N_2+1,\dots,N_2-1$.
FWD.1.3 Computation of the temperature at the new grid $G(t_l)$:

$$\hat{u}_{ij}^{(k)}(t_l) = \hat{u}_{ij}^{(k)}(t_{l-1}) + D_{s/l}\widehat{\Delta}\hat{u}_{ij}^{(k)}(t_{l-1})\tau + \hat{\partial}_{e_2}\hat{u}_{ij}^{(k)}(t_{l-1})(x_{ij,2}^{(k)}(t_l) - x_{ij,2}^{(k)}(t_{l-1}))$$

for $i = 1,\ldots,N_1 - 1$ and $|j| = 1,\ldots,N_2 - 1$. The terms $\widehat{\Delta}u_{ij}^{(k)}(t_{l-1})$ and $\hat{\partial}_{e_2}u_{ij}^{(k)}(t_{l-1})$ denote the finite difference approximation of Δu and $\partial_{e_2}u$ at $(t_{l-1}, x_{ij}^{(k)}(t_{l-1}))$.

FWD.1.4 Setting of the boundary values:

$$\hat{u}_{ij}^{(k)}(t_l) = u_b(t_l, x_{ij}^{(k)}(t_l)) + \beta_{l,ij}^{(k)}\hat{u}_{bc,ij}^{(k)}(t_l) \mp \frac{k_{s/l}}{\alpha_{s/l}}\hat{\partial}_{e_1}u_{ij}^{(k)}(t_l)$$

$$\text{for } i = 0, N_1 \text{ and } j = -N_2 + 1,\ldots,N_2 - 1,$$

$$\hat{u}_{ij}^{(k)}(t_l) = u_b(t_l, x_{ij}^{(k)}(t_l)) + \beta_{l,ij}^{(k)}\hat{u}_{bc,ij}^{(k)}(t_l) \pm \frac{k_{s/l}}{\alpha_{s/l}}\hat{\partial}_{e_2}u_{ij}^{(k)}(t_l)$$

$$\text{for } j = \pm N_2 \text{ and } i = 1,\ldots,N_1 - 1,$$

where $\beta_{l,ij}^{(k)} = \beta(x_{ij}^{(k)}(t_l))$.

The first equation in step FWD.1.1 is the discrete version of the Stefan condition (18) together with $\partial_\mu u = \partial_{e_2}u\sqrt{1+f_y}$. For the computation of the finite differences of the u-derivatives in step FWD.1.3 it has to be considered, that the grid in general is not orthogonal. The grid line $\{\hat{x}_{i0}^{(k)}(t_l)\}$ defines the discrete free boundary: $\hat{x}_{i0,2}^{(k)}(t_l) = \hat{f}_i^{(k)}(t_l)$. Both, in the solid phase (between 0 and $\hat{f}_i^{(k)}(t_l)$) and in the liquid phase (between $\hat{f}_i^{(k)}(t_l)$ and X_2) the grid points are distributed equidistantly in e_2 direction, see Fig. 2.

3.2. BWD: Backward step k

For the backward problem the same grid $\{x_{ij}^{(k-1)}(t_l)\}$ as for the (previous) forward problem is used.

BWD.0: Initialization of the adjoint temperatures:

$$\hat{q}_{s,ij}^{(k)}(T) = 0 \quad \text{for } i = 0,\ldots,N_1,\ j = -N_2,\ldots,-1,$$

$$\hat{q}_{l,ij}^{(k)}(T) = 0 \quad \text{for } i = 0,\ldots,N_1,\ j = 1,\ldots,N_2,$$

$$\hat{q}_{\Gamma,i}^{(k)}(T) = \lambda_2(\bar{f}(T,y_i) - \hat{f}_i^{(k-1)}(T)) \quad \text{for } i = 0,\ldots,N_1.$$

BWD.1: For all $l = N_t - 1,\ldots,0$

BWD.1.1 Setting of the adjoint temperatures $\hat{q}_s^{(k)}$ and $\hat{q}_l^{(k)}$ at the free boundary:

$$\hat{q}_{s,i0}^{(k)}(t_{l+1}) = \hat{q}_{\Gamma,i}(t_{l+1}),$$

$$\hat{q}_{l,i0}^{(k)}(t_{l+1}) = \hat{q}_{\Gamma,i}(t_{l+1}).$$

$\hat{\partial}_{e_2}^{\pm}\hat{u}_{i0}^{(k)}(t_{l-1})$ denote the finite forward/backward differences, as described above.

BWD.1.2 Computation of the adjoint temperature within the phases:

$$\hat{q}_{s,ij}^{(k)}(t_l) = \hat{q}_{s,ij}^{(k)}(t_{l+1}) + D_s\widehat{\Delta}\hat{q}_{s,ij}^{(k)}(t_{l+1})\tau + \hat{\partial}_{e_2}\hat{q}_{s,ij}^{(k)}(t_{l+1})\left(x_{ij,2}^{(k-1)}(t_l) - x_{ij,2}^{(k-1)}(t_{l+1})\right),$$

$$\hat{q}_{l,ij}^{(k)}(t_l) = \hat{q}_{l,ij}^{(k)}(t_{l+1}) + D_s\widehat{\Delta}\hat{q}_{l,ij}^{(k)}(t_{l+1})\tau + \hat{\partial}_{e_2}\hat{q}_{l,ij}^{(k)}(t_{l+1})\left(x_{ij,2}^{(k-1)}(t_l) - x_{ij,2}^{(k-1)}(t_{l+1})\right),$$

As in the forward algorithm, $\widehat{\Delta}\hat{q}$ denotes the finite difference approximation of Δq.

BWD.1.3 Setting of the boundary values:

$$\hat{q}^{(k)}_{s,ij}(t_1) = \mp\frac{k_s}{\alpha_s}\hat{\partial}_{e_1} q^{(k)}_{s,ij}(t_1) \quad \text{for } i = 0, N_1 \text{ and } j = 1,\dots,N_2-1,$$

$$\hat{q}^{(k)}_{s,ij}(t_1) = \frac{k_s}{\alpha_s}\hat{\partial}_{e_2} q^{(k)}_{s,ij}(t_1) \quad \text{for } j = -N_2 \text{ and } i = 1,\dots,N_1-1,$$

$$\hat{q}^{(k)}_{l,ij}(t_1) = \mp\frac{k_l}{\alpha_l}\hat{\partial}_{e_1} q^{(k)}_{l,ij}(t_1) \quad \text{for } i = 0, N_1 \text{ and } j = -N_2+1,\dots,-1,$$

$$\hat{q}^{(k)}_{l,ij}(t_1) = -\frac{k_l}{\alpha_l}\hat{\partial}_{e_2} q^{(k)}_{l,ij}(t_1) \quad \text{for } j = N_2 \text{ and } i = 1,\dots,N_1-1.$$

BWD.1.4 Computation of the adjoint temperature q_Γ:

$$\hat{q}^{(k)}_{\Gamma,i}(t_1) = \hat{q}^{(k)}_{\Gamma,i}(t_{l+1}) + \tau\left(\hat{f}^{(k-1)}_i(t_1) - \bar{f}(t_1, y_i)\right)$$

for $i = 1,\dots,N_1-1$. Setting of the boundary values

$$\hat{q}^{(k)}_{\Gamma,0}(t_1) = \hat{q}^{(k)}_{\Gamma,N_1}(t_1) = 0.$$

3.3. GRD: computation of the gradient

The numerical approximation of the gradient is computed according to (35);

GRD: Computation of the gradient:

$$\hat{v}^{(k)}_{ij}(t_1) = \lambda_1 \beta^{(k)2}_{l,ij} u^{(k-1)}_{\mathrm{bc},ij}(t_1) - \begin{cases} \alpha_s \beta^{(k)}_{l,ij} q^{(k)}_{s,ij}(t_1) & \text{for } i = 0, N_1 \text{ and } j = 1,\dots,N_2, \\ \alpha_s \beta^{(k)}_{l,ij} q^{(k)}_{s,ij}(t_1) & \text{for } j = -N_2 \text{ and } i = 0,\dots,N_1, \\ 0 & \text{for } j = 0 \text{ and } i = 0, N_1, \\ \alpha_l \beta^{(k)}_{l,ij} q^{(k)}_{l,ij}(t_1) & \text{for } i = 0, N_1 \text{ and } j = -N_2,\dots,-1, \\ \alpha_l \beta^{(k)}_{l,ij} q^{(k)}_{l,ij}(t_1) & \text{for } j = N_2 \text{ and } i = 0,\dots,N_1 \end{cases}$$

and for $l = 1,\dots,N_t$.

3.4. LM: line minimization

We use a quadratic approximation approach for line minimization of

$$s^{(k)} = \operatorname{argmin} K(s) \quad \text{where } K(s) := K\left(\hat{u}^{(k-1)}_{\mathrm{bc}} + s\hat{v}^{(k)}\right).$$

If we would evaluate K on the same grid as the one used for the forward and backward step, the line minimization would require the main part of the computation time. Numerical experience shows that high accuracy of $s^{(k)}$ is not required. Therefore in line minimization we evaluate K on a grid which is twice as coarse as the grid used for the forward and backward step. This increases the computational speed by a factor of eight. With $\breve{K}$ we denote the discrete version of K computed on the coarse grid.

LM.0: Choose three initial values: $s_{0,0}^{(k)} < s_{1,0}^{(k)} < s_{2,0}^{(k)}$
LM.1: For all $l = 1, \ldots, l_{\max}$

LM.1.1: Determine the quadratic function

$$q \in \Pi_2 \quad \text{satisfying } q\left(s_{i,l-1}^{(k)}\right) = \breve{K}\left(s_{i,l-1}^{(k)}\right) \quad \text{for } i = 0, 1, 2$$

and set

$$s_1^{(k)} = \operatorname{argmin}_{s \geqslant 0} q(s).$$

LM.1.2: Set the new support points: if $s_1^{(k)} < s_{0,l-1}^{(k)}$:

$$s_{0,l}^{(k)} = s_1^{(k)} \quad s_{1,l}^{(k)} = s_{0,l-1}^{(k)} \quad s_{2,l}^{(k)} = s_{2,l-1}^{(k)},$$

else if $s_{0,l-1}^{(k)} \leqslant s_1^{(k)} < s_{1,l-1}^{(k)}$:

$$s_{0,l}^{(k)} = s_{0,l-1}^{(k)} \quad s_{1,l}^{(k)} = s_1^{(k)} \quad s_{2,l}^{(k)} = s_{1,l-1}^{(k)},$$

else if $s_{1,l-1}^{(k)} \leqslant s_1^{(k)} < s_{2,l-1}^{(k)}$:

$$s_{0,l}^{(k)} = s_{1,l-1}^{(k)} \quad s_{1,l}^{(k)} = s_{1,l-1}^{(k)} \quad s_{2,l}^{(k)} = s_{2,l-1}^{(k)},$$

else

$$s_{0,l}^{(k)} = s_{0,l-1}^{(k)} \quad s_{1,l}^{(k)} = s_{2,l-1}^{(k)} \quad s_{2,l}^{(k)} = s_1^{(k)},$$

LM.1.3: if $s_{2,l}^{(k)} - s_{0,l}^{(k)} < \varepsilon\left(|s_{0,l}^{(k)}| + |s_{2,l}^{(k)}|\right)$ then GOTO LM.2
LM.2: Setting $s^{(k)}$ to the last minimum in LM.1.1: $s^{(k)} = s_1^{(k)}$

3.5. Discussion of Eqs. (7)–(13)

Enforcing $f(t,0) = \bar{f}(t,0)$ and $f(t,X_1) = \bar{f}(t,X_1)$ in (7) simplifies the numerical implementation. With this setting the grid points at the container boundary $x_{ij}^{(k)}$ with $i = 0, N_1$ or $|j| = N_2$ are known a priori (this means, that they are independent of the gradient iteration k, unlike the grid points on the rest of the grid). This allows us to use these grid points for the discretization of the container boundary, because these points have to be specified a priori in order to store the data, e.g. for $\hat{u}_{\mathrm{bc}}^{(k)}$ and $\hat{v}^{(k)}$.

4. Numerical results

4.1. Test problem

As test configuration for our optimal control approach we consider a container of the size 20 cm × 40 cm filled with a silicon melt. We optimize the solidification process over the time period $[0, T]$ with $T = 3600$. The physical constants for silicon are listed in Table 1. For $\alpha_{\mathrm{s/l}}$ we choose

$$\alpha_{\mathrm{s}} = 0.1\ \frac{\mathrm{J}}{\mathrm{s\ cm^2\ K}} \quad \text{and} \quad \alpha_{\mathrm{l}} = 0.05\ \frac{\mathrm{J}}{\mathrm{s\ cm^2\ K}}.$$

The desired free boundary is the moving line $\bar{f}(t,y) = 10 + \frac{1}{180}t$. As initial condition for the temperature we choose

$$u_0(x) = u'_{\mathrm{s/l}}(x_2 - 10) \quad \text{for } x = (x_1, x_2) \in \Omega_{\mathrm{s/l}}, \tag{42}$$

Table 1
Physical constants for silicon

$\rho = 2.5\ \frac{\mathrm{g}}{\mathrm{cm}^3}$	
$c_\mathrm{s} = 0.98\ \frac{\mathrm{J}}{\mathrm{g\ K}}$	$c_\mathrm{l} = 2.3\ \frac{\mathrm{J}}{\mathrm{g\ K}}$
$k_\mathrm{s} = 0.56\ \frac{\mathrm{J}}{\mathrm{s\ cm\ K}}$	$k_\mathrm{l} = 0.22\ \frac{\mathrm{J}}{\mathrm{s\ cm\ K}}$
$L = L_\mathrm{l} - L_\mathrm{s} = 16.4\ \frac{\mathrm{J}}{\mathrm{g}}$	
$\vartheta_\mathrm{M} = 1420\ ^\circ\mathrm{C}$	

where u'_s and u'_l are defined by

$$u'_{\mathrm{s/l}} := \frac{\alpha_{\mathrm{s/l}}}{180 k_{\mathrm{s/l}}(\alpha_\mathrm{s} - \alpha_\mathrm{l})}.$$

For the boundary value $u_{\mathrm{b}0}$ we choose

$$u_{\mathrm{b}0}(t,x) = u'_{\mathrm{s/l}}(x_2 - \bar{f}(t,0)) + v^T e_2 \frac{k_{\mathrm{s/l}}}{\alpha_{\mathrm{s/l}}} u'_{\mathrm{s/l}} \tag{43}$$

for $x \in \partial\Omega$ and $t \in [0,T]$.

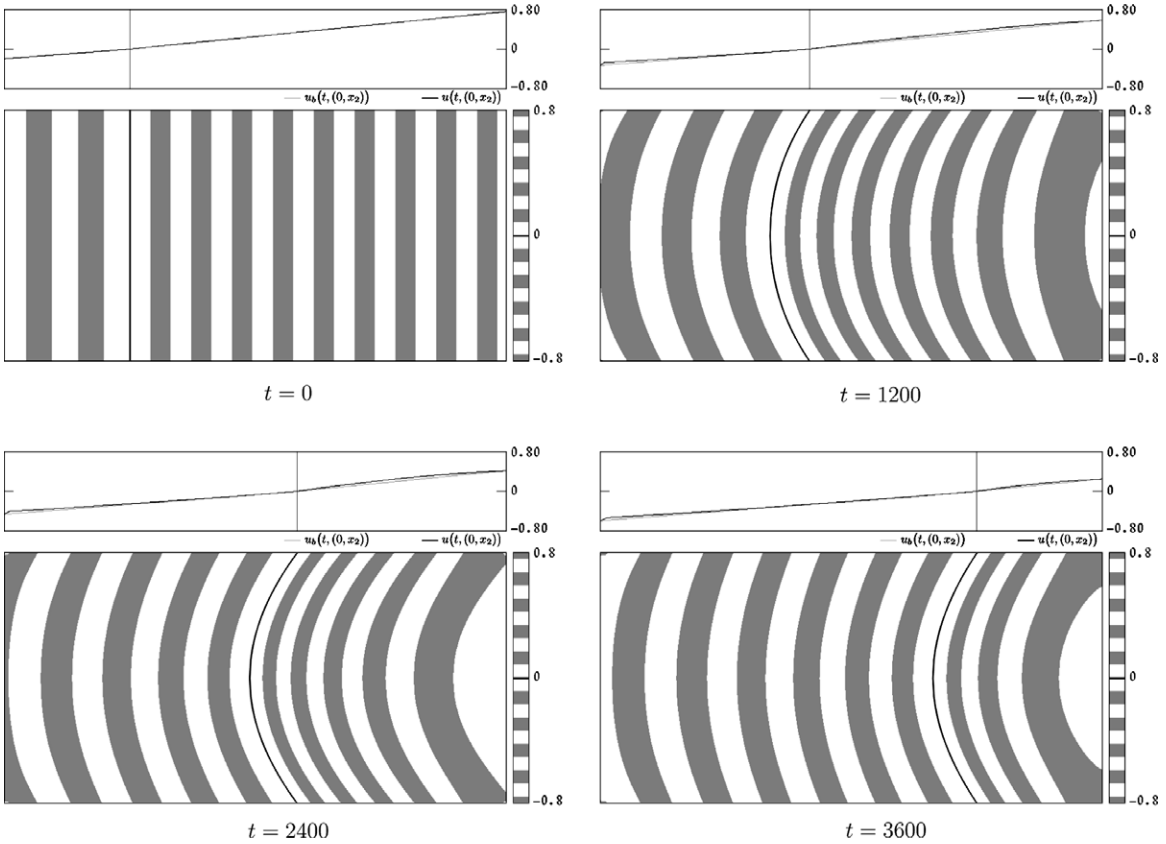

Fig. 3. The temperature u (white and grey stripes) and the free boundary (black line), together with the temperatures $u(t,(0,x_2))$ (black graph) and $u_\mathrm{b}(t,(0,x_2))$ (grey graph) at four different time instances for the uncontrolled problem ($u_\mathrm{bc} = 0$).

For this choice of $\bar{f}$ the function u_{b0} in (43) satisfies the compatibility conditions (8), (9), (11), (12) and (14). For β we consider the two cases

$$\beta_1(t,(0,x_2)) = \beta_1(t,(X_1,x_2)) = \begin{cases} \frac{tx_2(\bar{f}(t,0)-x_2)^2}{T\bar{f}(t,0)^3} & : x_2 < \bar{f}(t,0), \\ \frac{t(x_2-\bar{f}(t,0))^2(X_2-x_2)}{T(X_2-\bar{f}(t,0))^3} & : x_2 \geqslant \bar{f}(t,0), \end{cases}$$

$$\beta_1(t,(x_1,0)) = \beta_1(t,(x_1,X_2)) = \frac{t\sqrt{x_1(X_1-x_1)}}{TX_1},$$

and

$$\beta_2(t,(0,x_2)) = \beta_2(t,(X_1,x_2)) = \begin{cases} \frac{t}{T}\min\left\{1, 2\frac{(\bar{f}(t,0)-x_2)^2}{\bar{f}(t,0)^2}\right\} & : x_2 < \bar{f}(t,0), \\ \frac{t}{T}\min\left\{1, 2\frac{(x_2-\bar{f}(t,0))^2}{(X_2-\bar{f}(t,0))^2}\right\} & : x_2 \geqslant \bar{f}(t,0), \end{cases}$$

$$\beta_2(t,(x_1,0)) = \beta_2(t,(x_1,X_2)) = \frac{t}{T}$$

for $x_1 \in [0,X_1]$ and $x_2 \in [0,X_2]$. We note that both these choices of β satisfy (15).

At the corners $(0,0)$, $(0,X_2)$, $(X_1,0)$ and (X_1,X_2) of the domain the function β_1 is equal to 0. This means, that we enforce $u_{bc} = 0$ at these points. This prevents large boundary temperatures u_b, i.e. the choice of $\beta = \beta_1$ admits the flavour of a regularization of the problem. Therefore we set $\lambda_1 = 0$ in the case $\beta = \beta_1$. For $\beta = \beta_2$ we set $\lambda_1 = 1$.

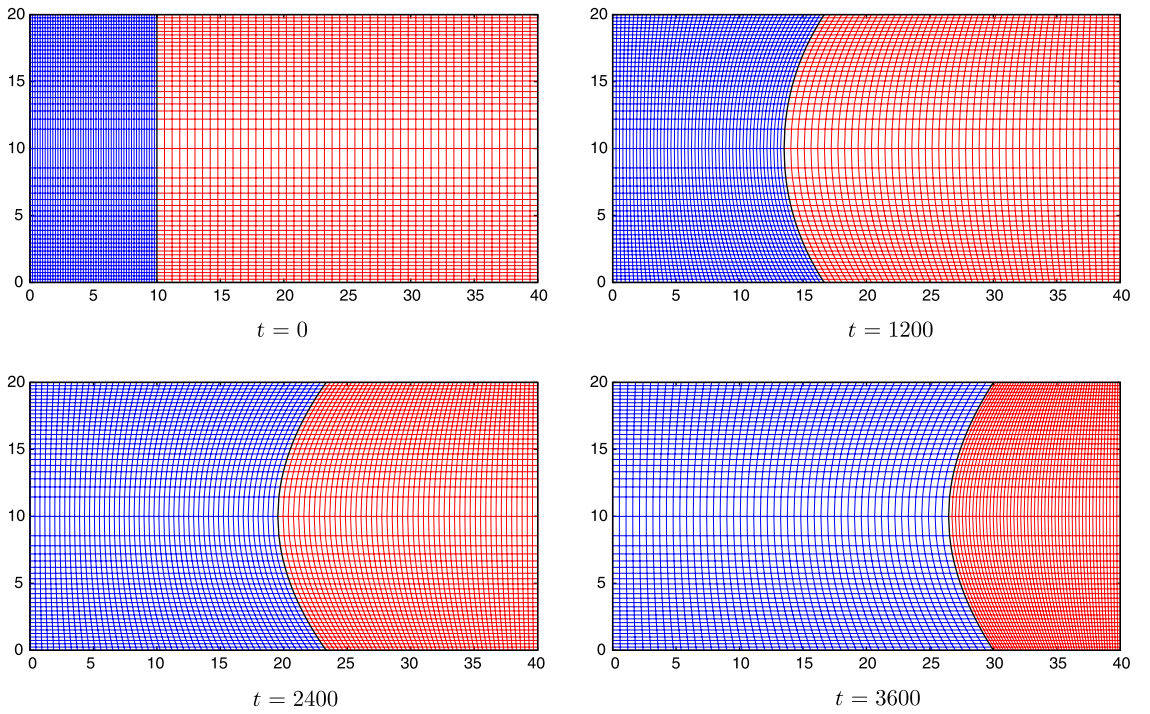

Fig. 4. The grid for the uncontrolled problem at four different time instances, see Fig. 3.

The spatial grid contains 51 points in e_1 direction and 101 points in e_2-direction. This implies $X_1 = X_2 = 50$. We set $\delta = 0.6$. The temporal grid contains 75001 grid points, i.e. $N_t = 75000$. This means that the number of optimization variables is approximately 4×10^8.

The computational time for one forward step (FWD) takes approximately 136 s on a single AMD Athlon MP 2133 MHz, for the backward step (BWD) it takes 133 s and the average computation time for one line minimization step (LM) is 142 s.

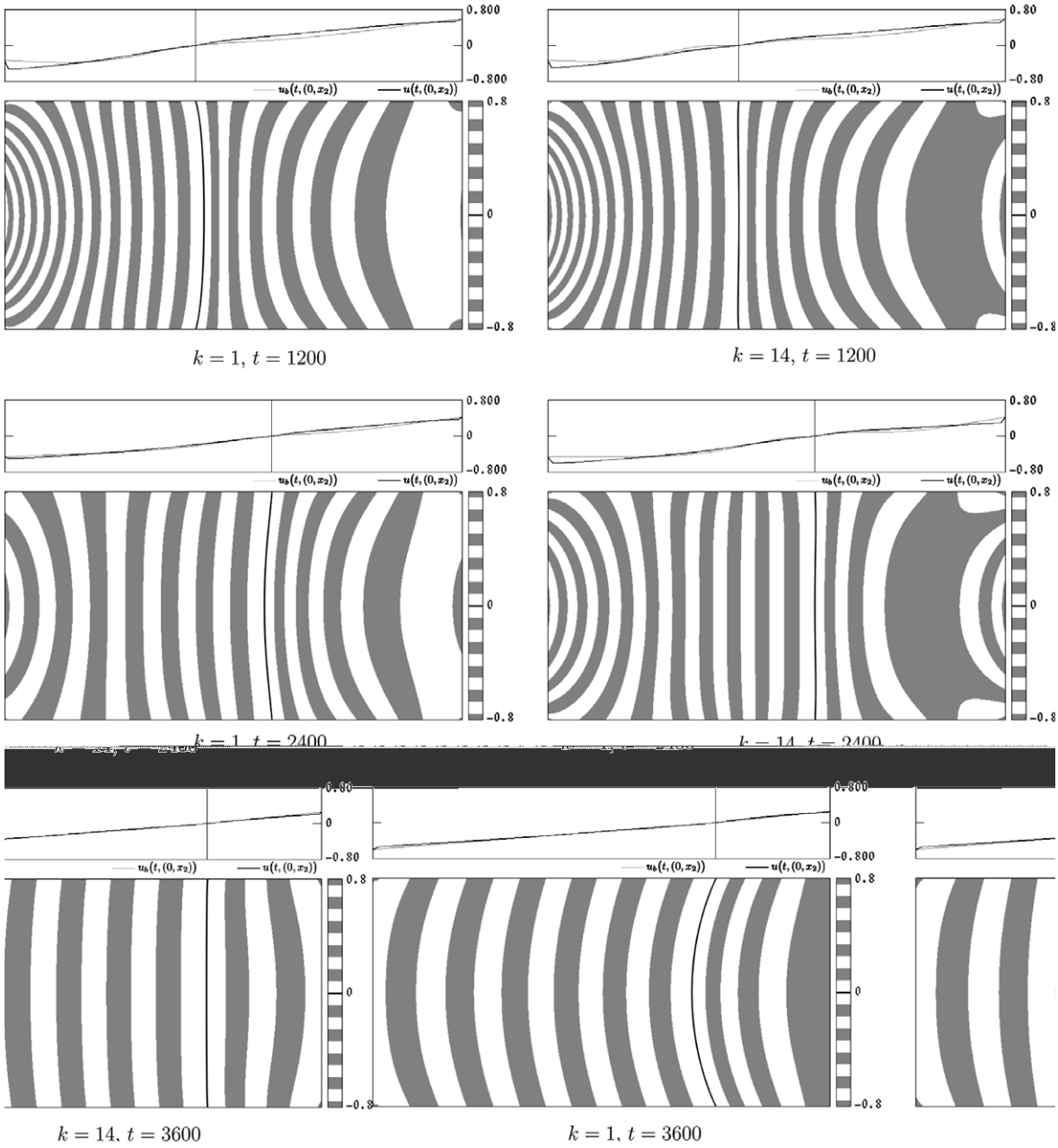

Fig. 5. The temperature u (white and grey stripes) and the free boundary (black line), together with the temperatures $u(t,(0,x_2))$ (black graph) and $u_b(t,(0,x_2))$ (grey graph). The images show the results for the case $\beta = \beta_1$ and $\lambda_1 = 0$ with $\lambda_2 = 0$ at three different time instances after the first gradient iteration (left) and after 14 gradient iterations, when the stopping criterion (40) is met.

4.2. Results for the uncontrolled case

First we examine the results for the uncontrolled forward problem with $u_{bc} = 0$ (Forward step 0 of the algorithm). Fig. 3 shows the shape of the free boundary, the temperature u and the graphs $u(t,(0,x_2))$ and $u_b(t,(0,x_2))$ with respect to x_2 at four different time instances, and Fig. 4 shows the corresponding grids. As expected forms the free boundary a concave graph during its evolution.

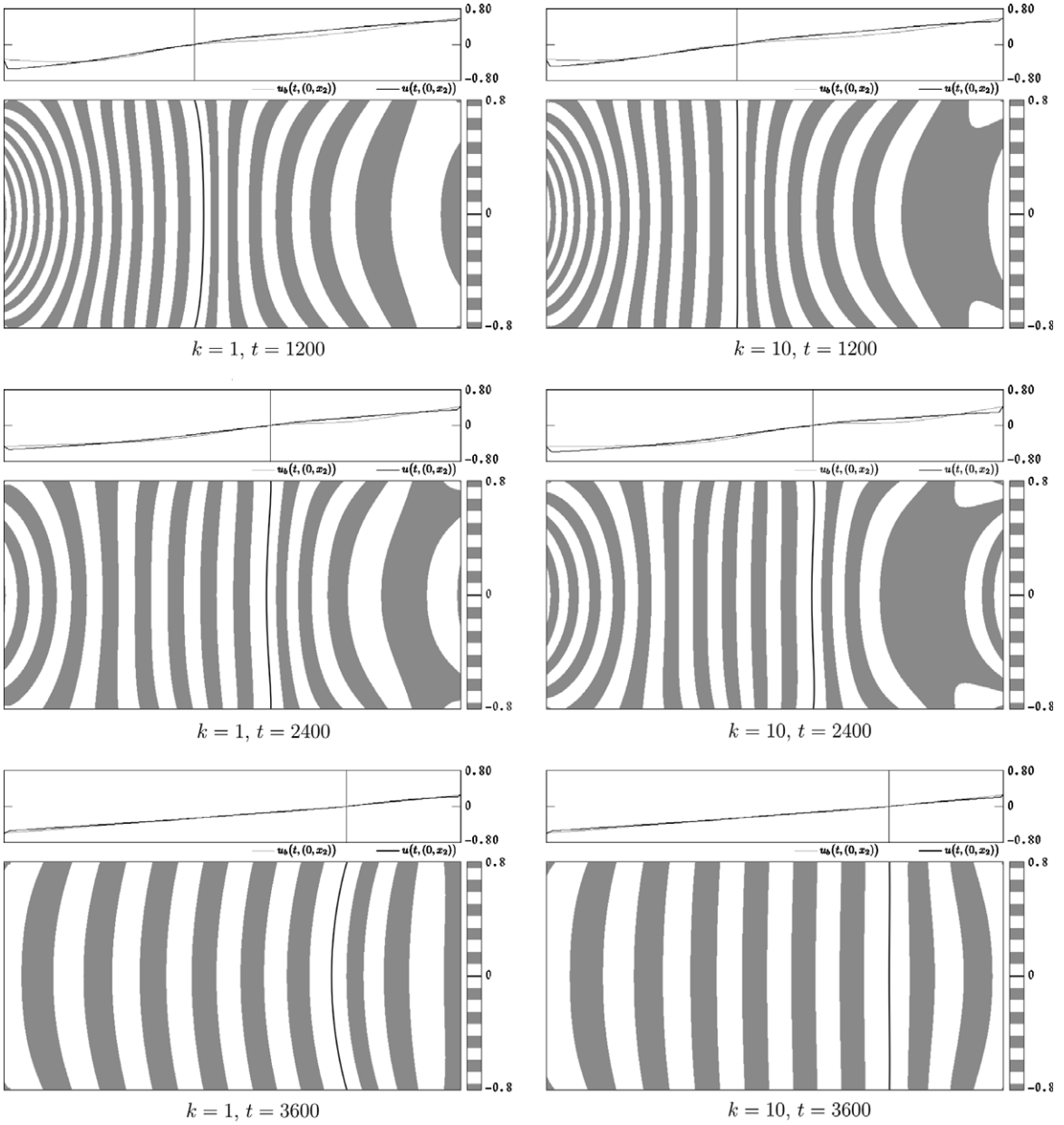

Fig. 6. The temperature u (white and grey stripes) and the free boundary (black line), together with the temperatures $u(t,(0,x_2))$ (black graph) and $u_b(t,(0,x_2))$ (grey graph). The images show the results for the case $\beta = \beta_1$ and $\lambda_1 = 0$ with $\lambda_2 = 500$ at three different time instances after the first gradient iteration (left) and after 10 gradient iterations, when the stopping criterion (40) is met. With $\lambda_2 = 500$ the error of the free boundary at time T is reduced quicker than with $\lambda_2 = 0$ (Fig. 5).

The temperature images (e.g. in Fig. 3) show white and grey stripes. Every stripe represents a temperature interval corresponding to the legend shown right. The black line depicts the free boundary. Above every temperature image two graphs are plotted. The black one shows the temperature $u(t,(0,x_2))$ and the grey graph represents the temperature $u_b(t,(0,x_2))$.

4.3. Results for the controlled case

Fist we examine the case $\beta = \beta_1$ and $\lambda_1 = 0$ for different weights λ_2. Later we compare these results with the results for the second case, $\beta = \beta_2$ and $\lambda_1 > 0$. We present results obtained after the first gradient iteration together with results obtained after the stopping criterion (40) is met, where we set $\varepsilon_J = 10^{-5}$. Finally we compare the numerical performance obtained with the stopping criterions (40) and (41).

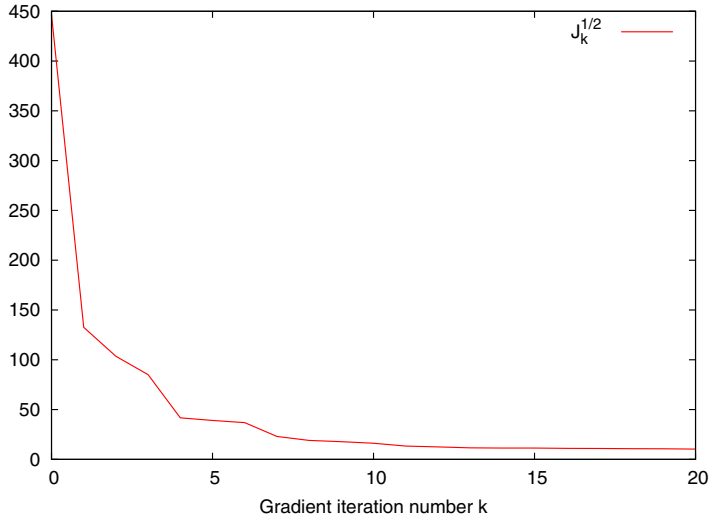

Fig. 7. Iteration history of $\sqrt{J}$ for the controlled problem with $\lambda_2 = 0$ for each gradient step k in the case $\beta = \beta_1$ and $\lambda_1 = 0$.

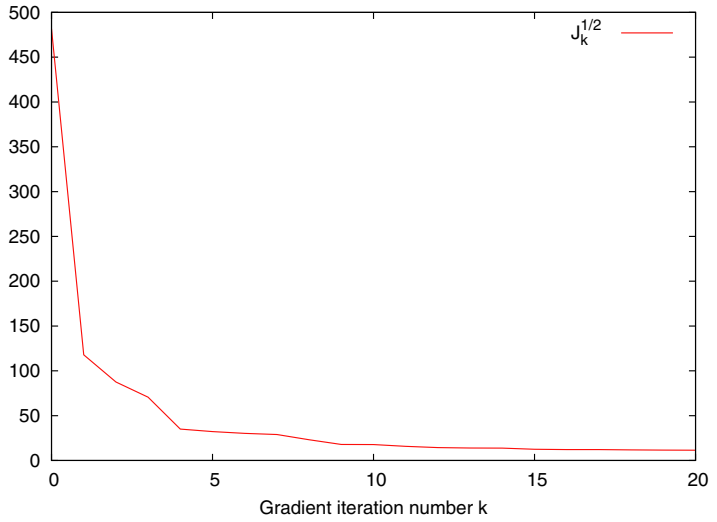

Fig. 8. Iteration history of $\sqrt{J}$ for the controlled problem with $\lambda_2 = 500$ for each gradient step k for the case $\beta = \beta_1$ and $\lambda_1 = 0$.

We begin our numerical investigation with the parameter setting $\beta = \beta_1$ and $\lambda_1 = \lambda_2 = 0$. This means that the error of the free boundary at time T is not penalized. As already noted in Section 4.1, we avoid large temperatures on the container wall by the choice of $\beta = \beta_1$, which allows us to set $\lambda_1 = 0$. Fig. 5 shows the shape of the free boundary, the temperature and the boundary temperature at three different time instances. (At $t = 0$ the temperature and the free boundary are equal to the temperature and free boundary, respectively of the

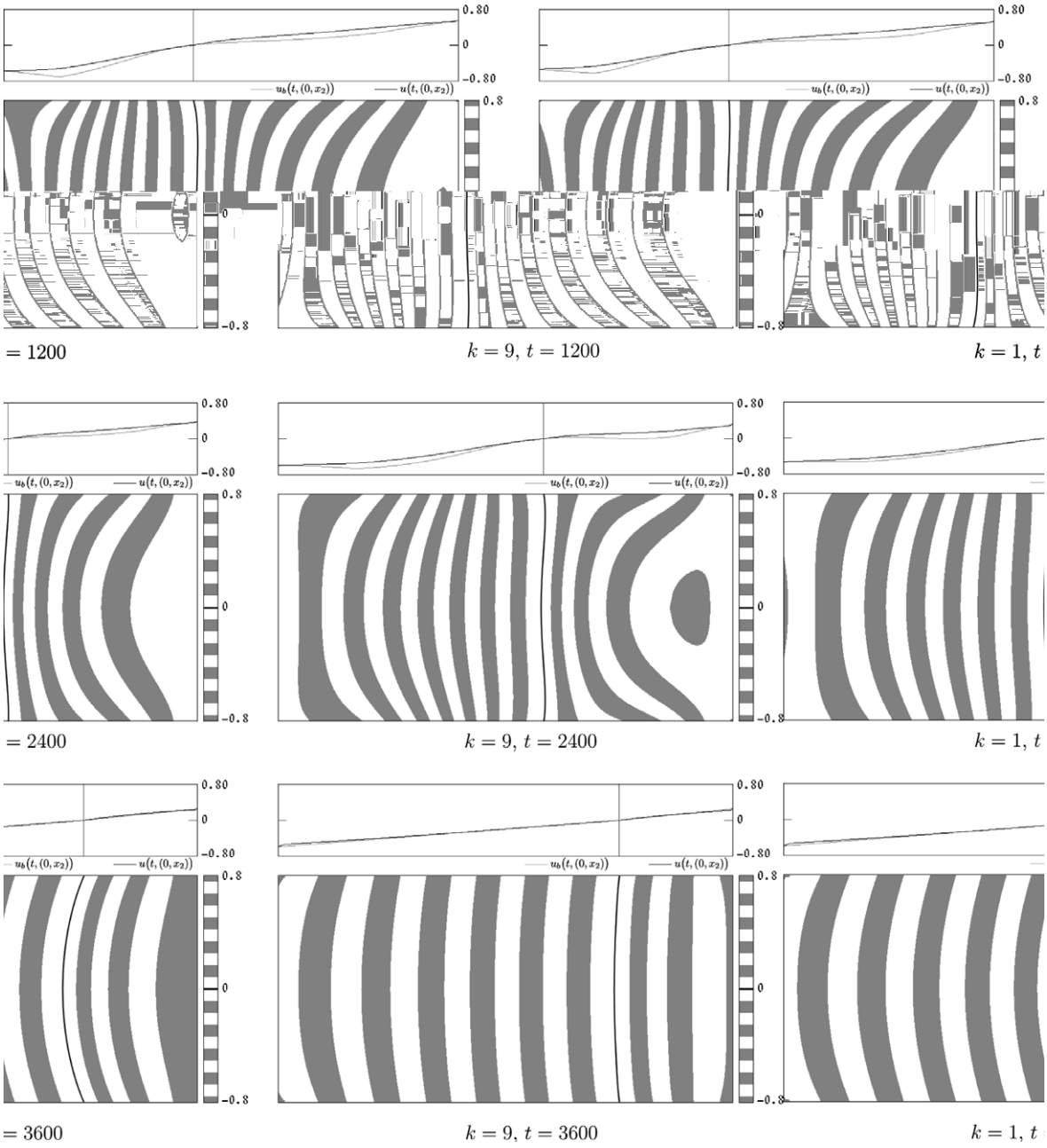

Fig. 9. The temperature u (white and grey stripes) and the free boundary (black line), together with the temperatures $u(t,(0,x_2))$ (black graph) and $u_b(t,(0,x_2))$ (grey graph). The images show the results for the case $\beta = \beta_2$ and $\lambda_1 = 1$ with $\lambda_2 = 500$ at three different time instances after the first gradient iteration and after nine gradient iterations, when the stopping criterion (40) is met.

uncontrolled problem.) Fig. 7 presents the cost functional J for every gradient iteration k. As can be seen the error

$$J_0 := \int_0^T \int_0^{X_1} (\bar{f}(t,y) - f(t,y))^2 \mathrm{d}x\,\mathrm{d}t, \tag{44}$$

is reduced very quickly, and that the optimized evolution of the free boundary delivers a nearly flat graph at all time instances.

Next, we set $\lambda_2 = 500$, $\beta = \beta_1$ and $\lambda_1 = 0$. The numerical results are presented in Fig. 8 (cost functional) and Fig. 6 (temperatures and free boundary). With this parameter choice

$$J_2 := \int_0^{X_1} (\bar{f}(T,y) - f(T,y))^2 \mathrm{d}x, \tag{45}$$

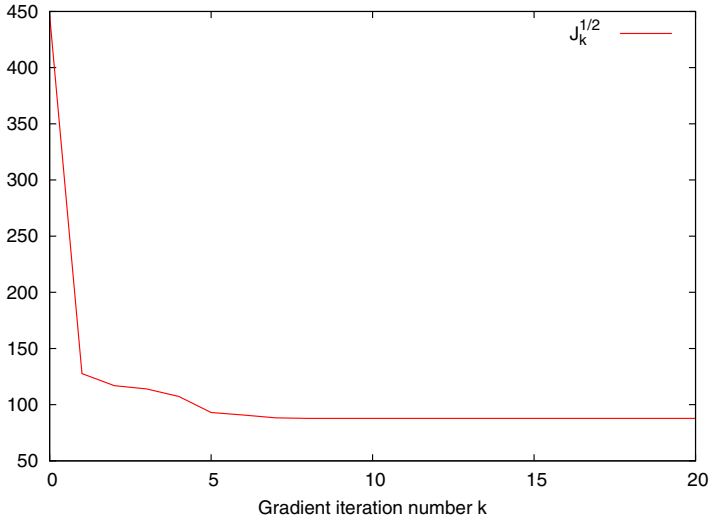

Fig. 10. Iteration history of $\sqrt{J}$ for the controlled problem with $\lambda_2 = 500$ for each gradient step k for the case $\beta = \beta_2$ and $\lambda_1 = 1$.

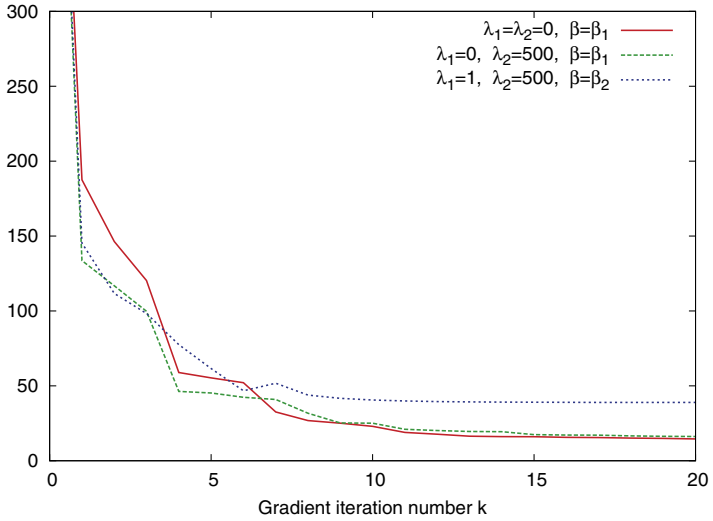

Fig. 11. Iteration history of the error of the free boundary $\sqrt{J_0}$ (compare (44)). In the cases $\lambda_1 = 0$ the function J_0 is reduced more, since these cases only deal with minimizing the error of the free boundary.

is penalized. As expected, our numerical algorithm quickly reduces this error, see Fig. 12, where the behaviour of this part of the functional is illustrated also for different parameter settings. The behaviour of J_0 for the same parameter settings is shown in Fig. 11. Again, the graph of the optimized evolution is nearly flat.

Now we investigate our second choice of β, i.e. we set $\beta = \beta_2$ and $\lambda_1 = 1$. Since effects due to λ_2 are similar to those in the case $\beta = \beta_1$, $\lambda_1 = 0$, we now fix $\lambda_2 = 500$. The temperatures are shown in Fig. 9 and the iteration history of the cost functional is presented in Fig. 10. With this parameter choice

$$J_1 = \int_0^T \int_{\partial\Omega} \beta(t,x)^2 u_{\mathrm{bc}}(t,x)^2 \mathrm{d}x\,\mathrm{d}t, \tag{46}$$

is penalized. In Figs. 11 and 12 it can be seen, that in the first gradient iterations the errors J_0 and J_2 of the free boundary are reduced as quick as in the case $\beta = \beta_1$, $\lambda_1 = 0$ with the same value for λ_2. But after approximately six iterations the errors J_0 and J_2 remain larger than in the cases $\beta = \beta_1$, $\lambda_1 = 0$. This can be explained by the fact that the setting $\lambda_1 = 1$ only allows smaller control actions as in the case $\lambda_1 = 0$. As a consequence the optimal evolution of the free boundary in the present case is not as flat as in the case $\beta = \beta_1$, $\lambda_1 = 0$.

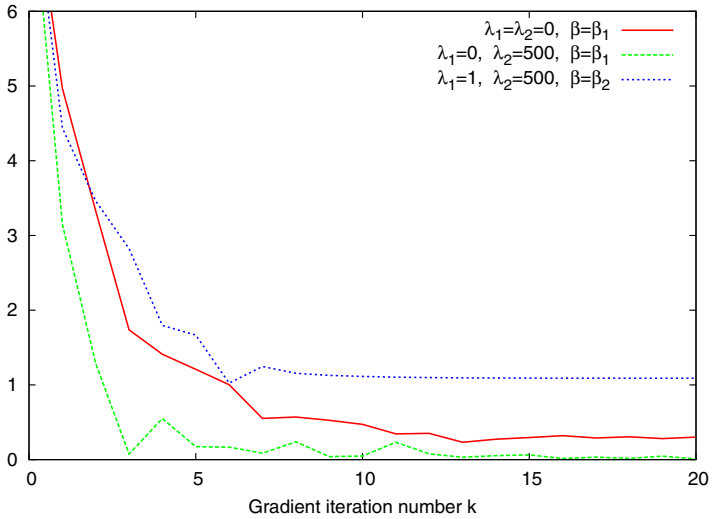

Fig. 12. Iteration history of the error of the free boundary $\sqrt{J_2}$ at time T (compare (45)). As expected, for $\lambda_2 > 0$ the functional J_2 is reduced most.

Table 2
The number of iterations $k_{\max}$ resulting from the stopping criterions (40) and (41) for all considered cases

β	β_1	β_1	β_2
λ_1	0	0	1
λ_2	0	500	500
$k_{\max}$	14	10	9

stopping criterion (40)

β	β_1	β_1	β_2
λ_1	0	0	1
λ_2	0	500	500
$k_{\max}$	12	10	9

stopping criterion (41)

As tolerances we set $\varepsilon_J = 10^{-5}$ and $\varepsilon_v = 10^{-3}$.

Table 2 shows the number of iterations $k_{\max}$ resulting from the stopping criterions (40) and (41). Using the first stopping criterion with $\varepsilon_J = 10^{-5}$ or the second one with $\varepsilon_v = 10^{-3}$ the algorithm converges quickly, and needs only about 10 iterations. With the choice $\lambda_2 = 500$ the algorithm converges a little bit faster than with $\lambda_2 = 0$.

With the tolerances $\varepsilon_J = 10^{-5}$ and $\varepsilon_v = 10^{-3}$ the iteration numbers $k_{\max}$ resulting from the stopping criterions (40) and (41) are very similar. For this reason we only present numerical results obtained with stopping criterion (40), see Figs. 5, 6 and 9.

As a result we note that with all investigated parameter constellations tracking of the desired evolution $\bar{f}$ works very well, see Figs. 5, 6 and 9. In particular we observe that the curvature of the optimized free boundary is in all considered cases close to zero.

5. Conclusion

We present control of solidification for a two-phase Stefan problem with sharp interface modeled as a graph. The control goal consists of tracking a prescribed evolution of the free boundary.

Our optimization approach ensures that the physical laws constituted by our mathematical model hold at every stage of the optimization process. This is accomplished by regarding the interface itself as optimization variable. We present several numerical examples which demonstrate the scope of our method. In all numerical investigations the tracking of the interface works very well.

The optimization procedure in all cases yields a boundary temperature distribution which quickly guarantees the desired flat free boundary.

We currently extend our approach to mathematical models which also incorporate flow driven by convection, and also include Lorentz forces as additional control variable. Further our approach easily extends to other physical models and/or other control configurations.

Acknowledgments

The authors acknowledge support of the Sonderforschungsbereich 609 *Elektromagnetische Strömungsbeeinflussung in Metallurgie, Kristallzüchtung und Elektrochemie* granted by the Deutsche Forschungsgemeinschaft.

Appendix A. Development of the adjoint equation system

The directive derivative of L with respect to u is equal to

$$L_u\tilde{u} = \int_0^T \int_{\Omega_s} (\partial_t\tilde{u} - D_s\Delta\tilde{u})p_s + \int_0^T \int_{\Omega_l} (\partial_t\tilde{u} - D_l\Delta\tilde{u})p_l + \int_0^T \int_0^{X_1} \left(\sqrt{1+f_y^2}[k_{s/l}\partial_\mu\tilde{u}] \circ \Phi\right)p_{\Gamma,1}$$
$$+ \int_0^T \int_0^{X_1} (\tilde{u} \circ \Phi)p_{\Gamma,2} + \int_0^T \int_{\partial\Omega_s(t)\setminus\Gamma(t)} \left(\frac{k_s}{\alpha_s}\partial_\nu\tilde{u} + \tilde{u}\right)p_{bs} + \int_0^T \int_{\partial\Omega_l(t)\setminus\Gamma(t)} \left(\frac{k_l}{\alpha_l}\partial_\nu\tilde{u} + \tilde{u}\right)p_{bl}.$$

Integration by parts of $\partial_t u$ with respect to t and of Δu with respect to x leads to

$$L_u\tilde{u} = \int_{\Omega_s} \tilde{u}(T,x)p_s(T,x)\mathrm{d}x - \int_{\Omega_s} \tilde{u}(0,x)p_s(0,x)\mathrm{d}x - \int_0^T \int_{\Omega_s} \tilde{u}\partial_t p_s - \int_0^T \int_{\partial\Omega_s\setminus\Gamma} D_s p_s \partial_\nu\tilde{u} - \int_0^T \int_\Gamma D_s p_s \partial_\nu\tilde{u}$$
$$+ \int_0^T \int_{\partial\Omega_s\setminus\Gamma} D_s\partial_\nu p_s\tilde{u} + \int_0^T \int_\Gamma D_s\partial_\nu p_s\tilde{u} - \int_0^T \int_{\Omega_s} D_s\tilde{u}\Delta p_s + \int_{\Omega_l} \tilde{u}(T,x)p_l(T,x)\mathrm{d}x$$
$$- \int_{\Omega_l} \tilde{u}(0,x)p_l(0,x)\mathrm{d}x - \int_0^T \int_{\Omega_l} \tilde{u}\partial_t p_l - \int_0^T \int_{\partial\Omega_l\setminus\Gamma} D_l p_l\partial_\nu\tilde{u} - \int_0^T \int_\Gamma D_l p_l\partial_\nu\tilde{u} + \int_0^T \int_{\partial\Omega_l\setminus\Gamma} D_l\partial_\nu p_l\tilde{u}$$

$$+\int_0^T\int_\Gamma D_l\partial_\nu p_l\tilde{u}-\int_0^T\int_{\Omega_l}D_l\tilde{u}\Delta p_l+\int_0^T\int_0^{X_1}\left(\sqrt{1+f_y'^2}[k_{s/l}\partial_\mu\tilde{u}]\circ\Phi\right)p_{\Gamma,1}$$
$$+\int_0^T\int_0^{X_1}(\tilde{u}\circ\Phi)p_{\Gamma,2}+\int_0^T\int_{\partial\Omega_s(t)\setminus\Gamma(t)}\left(\frac{k_s}{\alpha_s}\partial_\nu\tilde{u}+\tilde{u}\right)p_{bs}+\int_0^T\int_{\partial\Omega_l(t)\setminus\Gamma(t)}\left(\frac{k_l}{\alpha_l}\partial_\nu\tilde{u}+\tilde{u}\right)p_{bl}.$$

The temperature u must not vary at $t=0$, since u satisfies (21). This means that $\tilde{u}(0,x)$ has to vanish. Now we set $L_u\tilde{u}=0$ for all feasible directions $\tilde{u}$.

1a. We start with setting $L_u\tilde{u}=0$ for all $\tilde{u}$ with $\tilde{u}(t,x)=0$ and $\partial_\nu\tilde{u}(t,x)=0$ for $x\in\partial\Omega_s\cup\overline{\Omega_l}$ or $t=T$:

$$0=-\int_0^T\int_{\Omega_s}(\partial_t p_s+D_s\Delta p_s)\tilde{u}\Rightarrow\boxed{0=\partial_t p_s(t,x)+D_s\Delta p_s(t,x)}\quad\text{for } t\in(0,T)\text{ and } x\in\Omega_s(t).$$

1b. We set $L_u\tilde{u}=0$ for all $\tilde{u}$ with $\tilde{u}(t,x)=\partial_\nu\tilde{u}(t,x)=0$ for $x\in\partial\Omega_s\cup\partial\Omega_l$ or $t=T$. Considering the equation above we obtain

$$0=-\int_0^T\int_{\Omega_l}(\partial_t p_l+D_l\Delta p_l)\tilde{u}\Rightarrow\boxed{0=\partial_t p_l(t,x)+D_l\Delta p_l(t,x)}\quad\text{for } t\in(0,T)\text{ and } x\in\Omega_l(t).$$

2a. We set $L_u\tilde{u}=0$ for all $\tilde{u}$ with $\tilde{u}(t,x)=0$ for $x\in\partial\Omega_l$ or $t=T$ and $\partial_\nu\tilde{u}(t,x)=0$ for $x\in\partial\Omega_s\cup\partial\Omega_l$. Considering the equations above we obtain

$$0=\int_0^T\int_{\partial\Omega_s\setminus\Gamma}(D_s\partial_\nu p_s+p_{bs})\tilde{u}\Rightarrow p_{bs}(t,x)=-D_s\partial_\nu p_s(t,x)\quad\text{for } t\in(0,T)\text{ and } x\in\partial\Omega_s(t)\setminus\Gamma(t).$$

2b. We set $L_u\tilde{u}=0$ for all $\tilde{u}$ with $\tilde{u}(t,x)=0$ for $x\in\Gamma$ or $t=T$ and $\partial_\nu\tilde{u}(t,x)=0$ for $x\in\partial\Omega_s\cup\partial\Omega_l$. Considering the equations above we obtain

$$0=\int_0^T\int_{\partial\Omega_l\setminus\Gamma}(D_l\partial_\nu p_l+p_{bl})\tilde{u}\Rightarrow p_{bl}(t,x)=-D_l\partial_\nu p_l(t,x)\quad\text{for } t\in(0,T)\text{ and } x\in\partial\Omega_l(t)\setminus\Gamma(t).$$

3a. We set $L_u\tilde{u}=0$ for all $\tilde{u}$ with $\tilde{u}(t,x)=0$ for $x\in\Gamma$ or $t=T$ and $\partial_\nu\tilde{u}(t,x)=0$ for $x\in\partial\Omega_l$. Considering the equations above we obtain

$$0=\int_0^T\int_{\partial\Omega_s\setminus\Gamma}\left(-D_s p_s+\frac{k_s}{\alpha_s}p_{bs}\right)\partial_\nu\tilde{u}.$$

Substitution of $p_{bs}=-D_s\partial_\nu p_s$ (see 2a) leads to

$$\boxed{\begin{aligned}p_s(t,x)&=-\tfrac{k_s}{\alpha_s}\partial_\nu p_s(t,x)\\ p_{bs}(t,x)&=\tfrac{D_s\alpha_s}{k_s}p_s(t,x)\end{aligned}}\quad\text{for } t\in(0,T)\text{ and } x\in\partial\Omega_s(t)\setminus\Gamma(t).$$

3b. We set $L_u\tilde{u}=0$ for all $\tilde{u}$ with $\tilde{u}(t,x)=\partial_\nu\tilde{u}(t,x)=0$ for $x\in\Gamma$ or $t=T$. Considering the equations above we obtain:

$$0=\int_0^T\int_{\partial\Omega_l\setminus\Gamma}\left(-D_l p_l+\frac{k_l}{\alpha_l}p_{bl}\right)\partial_\nu\tilde{u}.$$

Substitution of $p_{bl}=-D_l\partial_\nu p_l$ (see 2b) leads to

$$\boxed{\begin{aligned}p_l(t,x)&=-\tfrac{k_l}{\alpha_l}\partial_\nu p_l(t,x)\\ p_{bl}(t,x)&=\tfrac{D_l\alpha_l}{k_l}p_l(t,x)\end{aligned}}\quad\text{for } t\in(0,T)\text{ and } x\in\partial\Omega_l(t)\setminus\Gamma(t).$$

4a. We set $L_u\tilde{u}=0$ for all $\tilde{u}$ with $\tilde{u}(t,x)=\partial_\nu\tilde{u}(t,x)=0$ for $x\in\Gamma$ or $(t,x)\in\{T\}\times\Omega_l(T)$. Considering the equations above we obtain

$$0=\int_{\Omega_s}\tilde{u}(T,x)p_s(T,x)\mathrm{d}x\Rightarrow\boxed{p_s(T,x)=0}\quad\text{for } x\in\Omega_s(T).$$

4b. We set $L_u\tilde{u} = 0$ for all $\tilde{u}$ with $\tilde{u}(t,x) = \partial_v\tilde{u}(t,x) = 0$ for $x \in \Gamma$. Considering the equations above we obtain

$$0 = \int_{\Omega_l} \tilde{u}(T,x)p_l(T,x)\mathrm{d}x \Rightarrow \boxed{p_l(T,x) = 0} \quad \text{for } x \in \Omega_l(T).$$

5a. We set $L_u\tilde{u} = 0$ for all $\tilde{u}$ with $(\tilde{u}\circ\Phi)(t,y) = 0$ and $(\partial_\mu\tilde{u}\circ\Phi)(t,y)|_{\Omega_s} = 0$ for $y \in (0,X_1)$ and $t \in (0,T)$. For the integrals over Γ we have to change the parametrization:

$$\int_\Gamma g = \int_0^{X_1} \|\Phi_y\|_2 \cdot g\circ\Phi = \int_0^{X_1} \sqrt{1+f_y^2}\cdot g\circ\Phi.$$

Considering this together with the equations above, we obtain

$$0 = \int_0^T \int_0^{X_1} \sqrt{1+f_y^2}(k_l p_{\Gamma,1} + D_l(p_l\circ\Phi))(\partial_\mu\tilde{u}|_{\Omega_l}\circ\Phi) \Rightarrow \boxed{p_{\Gamma,1}(t,y) = -\tfrac{D_l}{k_l}p_l(t,x)}$$

$$\text{for } t \in (0,t),\ y \in (0,X_1) \text{ and } x = \begin{pmatrix} y \\ f(t,y)\end{pmatrix}.$$

5b. We set $L_u\tilde{u} = 0$ for all $\tilde{u}$ with $(\tilde{u}\circ\Phi)(t,y) = 0$ for $y \in (0,X_1)$ and $t \in (0,T)$. Considering the equations above we obtain

$$0 = \int_0^T \int_0^{X_1} \sqrt{1+f_y^2}(-k_s p_{\Gamma,1} + D_s(p_s\circ\Phi))(\partial_\mu\tilde{u}|_{\Omega_l}\circ\Phi) \Rightarrow \boxed{p_{\Gamma,1}(t,y) = -\tfrac{D_s}{k_s}p_s(t,x)}$$

$$\text{for } t \in (0,t),\ y \in (0,X_1) \text{ and } x = \begin{pmatrix} y \\ f(t,y)\end{pmatrix}.$$

5c. We set $L_u\tilde{u} = 0$ for all $\tilde{u}$. Considering the equations above we obtain

$$0 = \int_0^T \int_0^{X_1} \left(\sqrt{1+f_y^2}(D_s\partial_v p_s\circ\Phi + D_l\partial_v p_l\circ\Phi) + p_{\Gamma,2}\right)\cdot(\tilde{u}\circ\Phi) \Rightarrow$$

$$\boxed{p_{\Gamma,2}(t,y) = \sqrt{1+f_y^2}[D_{s/l}\partial_\mu p_{s/l}]\left(t,\begin{pmatrix} y \\ f(t,y)\end{pmatrix}\right)} \quad \text{for } y \in (0,X_1) \text{ and } t \in (0,t).$$

With the substitutions (25) the adjoint equation system (26)–(31) follows.

As next we reassemble the Lagrange function by integration by parts (similar as $L_u\tilde{u}$):

$$\begin{aligned}
L = {} & \frac{1}{2}\int_0^T\int_0^{X_1}(f-\bar{f})^2 + \frac{\lambda_1}{2}\int_0^T\int_{\partial\Omega}\beta^2u_{bc}^2 + \frac{\lambda_2}{2}\int_0^{X_1}(f(T,y)-\bar{f}(T,y)l)^2\mathrm{d}y + \int_{\Omega_s}u(T,x)p_s(T,x)\mathrm{d}x \\
& - \int_{\Omega_s}u(0,x)p_s(0,x)\mathrm{d}x - \int_0^T\int_{\Omega_s}u\partial_t p_s - \int_0^T\int_{\partial\Omega_s\setminus\Gamma}D_s p_s\partial_v u - \int_0^T\int_\Gamma D_s p_s\partial_v u + \int_0^T\int_{\partial\Omega_s\setminus\Gamma}D_s\partial_v p_s u \\
& + \int_0^T\int_\Gamma D_s\partial_v p_s u - \int_0^T\int_{\Omega_s}D_s u\Delta p_s + \int_{\Omega_l}u(T,x)p_l(T,x)\mathrm{d}x - \int_{\Omega_l}u(0,x)p_l(0,x)\mathrm{d}x - \int_0^T\int_{\Omega_l}u\partial_t p_l \\
& - \int_0^T\int_{\partial\Omega_l\setminus\Gamma}D_l p_l\partial_v u - \int_0^T\int_\Gamma D_l p_l\partial_v u + \int_0^T\int_{\partial\Omega_l\setminus\Gamma}D_l\partial_v p_l u + \int_0^T\int_\Gamma D_l\partial_v p_l u - \int_0^T\int_{\Omega_l}D_l u\Delta p_l \\
& + \int_0^T\int_0^{X_1}\left(\sqrt{1+f_y^2}[k_{s/l}\partial_\mu u]\circ\Phi + f_t\right)p_{\Gamma,1} + \int_0^T\int_0^{X_1}(u\circ\Phi)p_{\Gamma,2} \\
& + \int_0^T\int_{\partial\Omega_s(t)\setminus\Gamma(t)}\left(\frac{k_s}{\alpha_s}\partial_v u + u - u_{b0} - \beta u_{bc}\right)p_{bs} + \int_0^T\int_{\partial\Omega_l(t)\setminus\Gamma(t)}\left(\frac{k_l}{\alpha_l}\partial_v u + u - u_{b0} - \beta u_{bc}\right)p_{bl}.
\end{aligned}$$

Substituting the already known parts of the adjoint equation system we obtain

$$L = \frac{1}{2}\int_0^T\int_0^{X_1}(f-\bar f)^2 + \frac{\lambda_1}{2}\int_0^T\int_{\partial\Omega}\beta^2 u_{\mathrm{bc}}^2 + \frac{\lambda_2}{2}\int_0^{X_1}(f(T,y)-\bar f(T,y))^2\mathrm{d}y - \int_{\Omega_\mathrm{s}} u(0,x)p_\mathrm{s}(0,x)\mathrm{d}x$$
$$- \int_{\Omega_\mathrm{l}} u(0,x)p_\mathrm{l}(0,x)\mathrm{d}x + \int_0^T\int_0^{X_1} f_t p_{\Gamma,1} + \int_0^T\int_{\partial\Omega_\mathrm{s}(t)\setminus\Gamma(t)}(-u_{\mathrm{b}0}-\beta u_{\mathrm{bc}})p_{\mathrm{bs}}$$
$$+ \int_0^T\int_{\partial\Omega_\mathrm{l}(t)\setminus\Gamma(t)}(-u_{\mathrm{b}0}-\beta u_{\mathrm{bc}})p_{\mathrm{bl}}.$$

The directional derivative with respect to f is equal to

$$L_f\tilde f = \int_0^T\int_0^{X_1}(f-\bar f)\tilde f + \lambda_2\int_0^{X_1} l(f(T,y)-\bar f(T,y))\tilde f(T,y)\mathrm{d}y + \int_0^T\int_0^{X_1}\tilde f_t p_{\Gamma,1}.$$

Integration by parts leads to

$$L_f\tilde f = \int_0^T\int_0^{X_1}(f-\bar f)\tilde f + \lambda_2\int_0^{X_1}(f(T,y)-\bar f(T,y))\tilde f(T,y)\mathrm{d}y + \int_0^{X_1} p_{\Gamma,1}(T,y)\tilde f(T,y)\mathrm{d}y$$
$$- \int_0^{X_1} p_{\Gamma,1}(0,y)\tilde f(0,y)\mathrm{d}y - \int_0^T\int_0^{X_1}\partial_t p_{\Gamma,1}\tilde f.$$

The function f must not vary at $t=0$, since f satisfies (22). This means that $\tilde f(0,y)$ vanish. We set $L_f\tilde f = 0$ for all feasible directions $\tilde f$.

1. We set $L_f\tilde f = 0$ for all $\tilde f$ with $\tilde f(T,y) = 0$ ($y\in[0,x_1]$). Considering the re-parametrization we obtain

$$0 = \int_0^T\int_0^{X_1}(f-\bar f-\partial_t p_{\Gamma,1})\tilde f \Rightarrow \boxed{-\partial_t p_{\Gamma,1} = \bar f(t,y) - f(t,y)} \quad \text{for } t\in(0,T) \text{ and } y\in(0,X_1).$$

2. Finally we set $L_f\tilde f = 0$ for all $\tilde f$. Considering the equations above we obtain

$$0 = \int_0^{X_1}(\lambda_2(f(T,y)-\bar f(T,y)) + p_{\Gamma,1}(T,y))\tilde f(T,y)\mathrm{d}y \Rightarrow \boxed{p_{\Gamma,1}(T,y) = \lambda_2(\bar f(T,y) - f(T,y))} \quad \text{for } y\in(0,X_1).$$

With the substitutions (25) the adjoint equation system (32)–(34) follows.

Appendix B. Compatibility conditions (8), (9), (11) and (12)

To derive (8), (9), (11) and (12) we assume continuity of our mathematical system at the intersection of the free boundary and the container wall. In the present two-dimensional setting we need to distinguish two cases, namely the intersection at $\{(0,f(t,0))\}$ and the intersection at $\{(X_1,f(t,X_1))\}$. Since these cases only differ in signs we distinguish between the two cases using "$\pm$" and "$\mp$", respectively, where the upper sign refers to the intersection at $\{(0,f(t,0))\}$ and the lower sign refers to the intersection at $\{(X_1,f(t,X_1))\}$.

Theorem B.1. *If $u(t,x)$, $u_b(t,x)$ and $\nabla u(t,x)$ are continuous with respect to x and $f_t(t,y)$ is continuous with respect to y, the following equations are satisfied on $(0,T]\times\{(0,f(t,0))\}$ and on $(0,T]\times\{(X_1,f(t,X_1))\}$, respectively;*

$$\frac{f_t f_y}{1+f_y^2} = \pm(\alpha_\mathrm{s}-\alpha_\mathrm{l})u_\mathrm{b}, \quad \textit{and} \tag{B.1}$$

$$\partial_{e_2}u_\mathrm{b}|_{\Omega_{\mathrm{s/l}}} = \frac{f_t}{1+f_y^2}g\left(\frac{1}{\alpha_\mathrm{s}-\alpha_\mathrm{l}}\left(\frac{\alpha_{\mathrm{s/l}}}{k_{\mathrm{s/l}}} \pm 2\frac{f_y f_{yy}}{(1+f_y^2)^2}\right) - \frac{u_\mathrm{b}}{D_{\mathrm{s/l}}}\right) \mp \frac{f_{yt}}{(\alpha_\mathrm{s}-\alpha_\mathrm{l})(1+f_y^2)^2}. \tag{B.2}$$

These form the compatibility conditions (8), (9), (11) and (12).

Proof of (B.1). Let us recall some identities for the normal vector at the free boundary and the temperature gradient at the container wall;

$$\mu = \frac{1}{\sqrt{1+f_y^2}}\begin{pmatrix} -f_y \\ 1 \end{pmatrix} \quad \nabla u = \begin{pmatrix} \partial_{e_1} u \\ \partial_{e_2} u \end{pmatrix} = \begin{pmatrix} \mp\partial_\nu u \\ \partial_{e_2} u \end{pmatrix}.$$

The tangential vector τ at the free boundary is given by

$$\tau = \frac{1}{\sqrt{1+f_y^2}}\begin{pmatrix} 1 \\ f_y \end{pmatrix}.$$

From the melting temperature condition $u = 0$ on the free boundary we obtain

$$\partial_\tau u = \frac{\mp\partial_\nu u|_{\Omega_{s/l}} + f_y \partial_{e_2} u|_{\Omega_{s/l}}}{\sqrt{1+f_y^2}} = 0,$$

which implies

$$\pm\partial_\nu u|_{\Omega_{s/l}} = f_y \partial_{e_2} u|_{\Omega_{s/l}}. \tag{B.3}$$

Using $\partial_\mu u = \frac{\pm f_y \partial_\nu u + \partial_{e_2} u}{\sqrt{1+f_y^2}}$ and (B.3) we obtain;

$$\frac{f_y \partial_\mu u|_{\Omega_{s/l}}}{\sqrt{1+f_y^2}} = \frac{\pm f_y^2 \partial_\nu u|_{\Omega_{s/l}} + f_y \partial_{e_2} u|_{\Omega_{s/l}}}{1+f_y^2} \underset{(B.3)}{=} \frac{\pm f_y^2 \partial_\nu u|_{\Omega_{s/l}} \pm \partial_\nu u|_{\Omega_{s/l}}}{1+f_y^2} = \pm\partial_\nu u|_{\Omega_{s/l}}. \tag{B.4}$$

From the boundary condition $u_b - u = \frac{k_{s/l}}{\alpha_{s/l}} \partial_\nu u|_{\Omega_{s/l}}$ and from $u = 0$ on the free boundary it follows that

$$u_b = \frac{k_{s/l}}{\alpha_{s/l}} \partial_\nu u|_{\Omega_{s/l}}. \tag{B.5}$$

Using the calculations above and substituting f_t by the Stefan condition (18) we finally obtain

$$\frac{f_y f_t}{1+f_y^2} \underset{\text{(Stefan cond.)}}{=} -k_l \frac{f_y \partial_\mu u|_{\Omega_l}}{\sqrt{1+f_y^2}} + k_s \frac{f_y \partial_\mu u|_{\Omega_s}}{\sqrt{1+f_y^2}} \underset{(B.4)}{=} \mp k_l \partial_\nu u|_{\Omega_l} \pm k_s \partial_\nu u|_{\Omega_s} \underset{(B.5)}{=} \pm(\alpha_s - \alpha_l) u_b,$$

which is (B.1). □

Proof of (B.2). By (B.3) and (B.4) we obtain

$$\frac{\partial_\mu u|_{\Omega_{s/l}}}{\sqrt{1+f_y^2}} = \partial_{e_2} u|_{\Omega_{s/l}}. \tag{B.6}$$

From the boundary condition $u_b = u + \frac{k_{s/l}}{\alpha_{s/l}} \partial_\nu u$ it follows that

$$\partial_{e_2} u_b|_{\Omega_{s/l}} = \partial_{e_2} u|_{\Omega_{s/l}} + \frac{k_{s/l}}{\alpha_{s/l}} \partial_{e_2} \partial_\nu u|_{\Omega_{s/l}}. \tag{B.7}$$

Thus we need to derive formulations for $\partial_{e_2} u$ and $\partial_{e_2}\partial_\nu u$. First we consider $\partial_{e_2} u$. From (B.4), (B.5) and (B.1) it follows that

$$\frac{f_y \partial_\mu u|_{\Omega_{s/l}}}{\sqrt{1+f_y^2}} \underset{(B.4)}{=} \pm\partial_\nu u|_{\Omega_{s/l}} \underset{(B.5)}{=} \pm\frac{\alpha_{s/l}}{k_{s/l}} u_b \underset{(B.1)}{=} \frac{\alpha_{s/l}}{(\alpha_s - \alpha_l) k_{s/l}} \cdot \frac{f_t f_y}{1+f_y^2},$$

which implies

$$\partial_\mu u|_{\Omega_{s/l}} = \frac{\alpha_{s/l}}{(\alpha_s - \alpha_l) k_{s/l}} \cdot \frac{f_t}{\sqrt{1+f_y^2}}. \tag{B.8}$$

From (B.6) we obtain

$$\partial_{e_2} u|_{\Omega_{s/l}} = \frac{\alpha_{s/l}}{(\alpha_s - \alpha_l)k_{s/l}} \cdot \frac{f_t}{1+f_y^2}. \tag{B.9}$$

The expression $\partial_v \partial_{e_2} u$ is composed of $\partial_\tau \partial_{e_2} u$ and $\partial_\mu \partial_{e_2} u$. In order to derive expressions for the latter quantities we need to provide derivatives in direction τ of re-parametrized variables of the form $g\left(\begin{pmatrix} y \\ f(y) \end{pmatrix}\right)$. Forming limits gives

$$\begin{aligned}\partial_\tau g\left(\begin{pmatrix} y \\ f(y) \end{pmatrix}\right) &= \lim_{\varepsilon \to 0} \frac{g\left(\begin{pmatrix} y \\ f(y) \end{pmatrix} + \frac{\varepsilon}{\sqrt{1+f_y^2}} \begin{pmatrix} 1 \\ f_y(y) \end{pmatrix}\right) - g\left(\begin{pmatrix} y \\ f(y) \end{pmatrix}\right)}{\varepsilon} = \lim_{\varepsilon \to 0} \frac{\frac{\varepsilon}{\sqrt{1+f_y^2}} \nabla g^T \begin{pmatrix} 1 \\ f_y \end{pmatrix}}{\varepsilon} \\ &= \frac{1}{\sqrt{1+f_y^2}} \partial_y g\left(\begin{pmatrix} y \\ f(y) \end{pmatrix}\right).\end{aligned}$$

Now the expression for $\partial_\tau \partial_{e_2} u$ follows from (B.9);

$$\partial_\tau \partial_{e_2} u|_{\Omega_{s/l}} = \frac{\alpha_{s/l}}{(\alpha_s - \alpha_l)k_{s/l}} \cdot \partial_y \left(\frac{f_t}{1+f_y^2}\right) \frac{1}{\sqrt{1+f_y^2}} = \frac{\alpha_{s/l}}{(\alpha_s - \alpha_l)k_{s/l}} \left(\frac{f_{ty}}{(1+f_y^2)^{1.5}} - 2\frac{f_t f_y f_{yy}}{(1+f_y^2)^{2.5}}\right). \tag{B.10}$$

From the heat equation at the free boundary ($\partial_\tau^2 u = 0$) and from (B.8) it follows that

$$D_{s/l} \partial_\mu^2 u|_{\Omega_{s/l}} = \partial_t u|_{\Omega_{s/l}} = -V_\Gamma \partial_\mu u|_{\Omega_{s/l}} = -\frac{f_t}{\sqrt{1+f_y^2}} \partial_\mu u|_{\Omega_{s/l}} \underset{(B.8)}{=} -\frac{\alpha_{s/l}}{(\alpha_s - \alpha_l)k_{s/l}} \cdot \frac{f_t^2}{1+f_y^2},$$

and by substitution of (B.6) we obtain

$$\partial_\mu \partial_{e_2} u|_{\Omega_{s/l}} = -\frac{\alpha_{s/l}}{(\alpha_s - \alpha_l)k_{s/l} D_{s/l}} \cdot \frac{f_t^2}{(1+f_y^2)^{1.5}}. \tag{B.11}$$

Finally we can derive an expression for $\partial_{e_2} \partial_v u$ from (B.10) and (B.11);

$$\begin{aligned}\partial_v \partial_{e_2} u|_{\Omega_{s/l}} &= v^T \tau \partial_\tau \partial_{e_2} u|_{\Omega_{s/l}} + v^T \mu \partial_\mu \partial_{e_2} u|_{\Omega_{s/l}} = \mp \left(\frac{1}{\sqrt{1+f_y^2}} \partial_\tau \partial_{e_2} u|_{\Omega_{s/l}} - \frac{f_y}{\sqrt{1+f_y^2}} v^T \mu \partial_\mu \partial_{e_2} u|_{\Omega_{s/l}}\right) \\ &= \mp \frac{\alpha_{s/l}}{(\alpha_s - \alpha_l)k_{s/l}} \left(\frac{f_{ty}}{(1+f_y^2)^2} - 2\frac{f_t f_y f_{yy}}{(1+f_y^2)^3} + \frac{1}{D_{s/l}} \cdot \frac{f_y f_t^2}{(1+f_y^2)^2}\right) \\ &\underset{(B.1)}{=} \mp \frac{\alpha_{s/l}}{k_{s/l}} \left(\frac{1}{\alpha_s - \alpha_l} \left(\frac{f_{ty}}{(1+f_y^2)^2} - 2\frac{f_t f_y f_{yy}}{(1+f_y^2)^3}\right) \pm \frac{u_b}{D_{s/l}} \cdot \frac{f_t}{1+f_y^2}\right).\end{aligned} \tag{B.12}$$

Now (B.2) can be assembled directly from (B.7), (B.9) and (B.12);

$$\partial_{e_2} u_b|_{\Omega_{s/l}} = \frac{f_t}{1+f_y^2} \left(\frac{1}{\alpha_s - \alpha_l} \left(\frac{\alpha_{s/l}}{k_{s/l}} \pm 2\frac{f_y f_{yy}}{(1+f_y^2)^2}\right) - \frac{u_b}{D_{s/l}} g\right) \frac{f_{yt}}{(\alpha_s - \alpha_l)(1+f_y^2)^2}. \qquad \square$$

References

[3] P. Colli, M. Grasselli, J. Sprekels, Automatic control via thermostats of a hyperbolic stefan problem with memory, Applied Mathematics and Optimization 39 (1999) 229–255.

[4] W.B. Dunbar, N. Petit, P. Rouchon, P. Martin, Boundary control of a nonlinear Stefan problem, in: Proceedings of the 2003 Conference on Decision and Control, Maui, HI, 2003, pp. 1309–1314.

[5] W.B. Dunbar, N. Petit, P. Rouchon, P. Martin, Motion planning for a nonlinear Stefan problem, Control Optimisation and Calculus of Variations 9 (2003) 275–296.

[6] K.-H. Hoffmann, J. Sprekels, Real-time control in a free boundary problem connected with the continuous casting of steel, in: K.-H. Hoffmann, W. Krabs (Eds.), Optimal Control of Partial Differential Equations, Birkhäuser, 1984.
[7] S. Kang, N. Zabaras, Control of the freezing interface motion in two-dimensional solidification processes using the adjoint method, International Journal for Numerical Methods in Engineering 38 (1995) 63–80.
[8] A.J. Kearsley, The use of optimization techniques in the solution of partial differential equations from science and engineering, PhD thesis, Rice University, 1996.
[9] T. Neunhoeffer, Numerische Simulation von Erstarrungsprozessen unterkühlter Flüssigkeiten unter Berücksichtigung von Dichteunterschieden, PhD thesis, Technische Universität München, Fakultät für Informatik, 1997.
[10] I. Pawlow, Optimal control of two-phase stefan problems – numerical solutions, in: K.-H. Hoffmann, W. Krabs (Eds.), Optimal Control of Partial Differential Equations II. Theory and Applications, Birkhäuser, 1987.
[11] I. Pawlow, Optimal control of dynamical processes in two-phase systems of solid–liquid type, Banach Center Publications 24 (1990) 293–319.
[15] A. Visintin, Models of Phase Transitions, Birkhäuser, 1996.
[16] Z. Yang, The adjoint method for the inverse design of solidification processes with convection, PhD thesis, Cornell University, 1997.
[17] N. Zabaras, Inverse problems in heat transfer, in: W.J. Minkowycz, E.M. Sparrow, J.Y. Murthy (Eds.), Handbook of Numerical Heat Transfer, second ed., John Wiley & Sons, 2004 (Chapter 17).
[18] N. Zabaras, S. Mukherjee, O. Richmond, An analysis of inverse heat transfer problems with phase changes using an integral method, Journal of Heat Transfer ASME 110 (1988) 554–561.
[19] N. Zabaras, T. Hung Nguyen, Control of the freezing interface morphology in solidification processes in the presence of natural convection, International Journal for Numerical Methods in Engineering 38 (1995) 1555–1578.
[20] N. Zabaras, Y. Ruan, O. Richmond, On the design of two-dimensional stefan processes with desired freezing front motions, Numerical Heat Transfer, Part B 21 (1992) 307–325.